Food Bioscience 84 (2026) 109748

Contents lists available at ScienceDirect

Food Bioscience

journal homepage: www.elsevier.com/locate/fbio

Integrated ultrasound-assisted enzymatic extraction from grape seeds: impact on oil yield, fatty acid profile, and antimicrobial activity

Alessia Di Fraia [a], Martina Aulitto [a], Danila Limauro [a], Vito Michele Paradiso [b], Armando Zarrelli [c], Gabriella Fiorentino [a,*]

[a] Department of Biology, University of Naples Federico II, Complesso Universitario Monte S. Angelo, Via Cinthia 4, Naples, 80126, Italy
[b] Department of Biological and Environmental Sciences and Technologies, University of Salento, S.P. 6, Lecce-Monteroni, Lecce, I-73100, Italy
[c] Department of Chemical Sciences, University of Naples Federico II, Complesso Universitario Monte S. Angelo, Via Cinthia 4, Naples, 80126, Italy

ARTICLE INFO

Keywords:
Enzyme-assisted extraction
Ultrasound technology
Grape seed oil
Fatty acid profile
Antimicrobial activity

ABSTRACT

Grape seeds recovered from grape marc distillation are rich in lipids, proteins, and carbohydrates, but their structured lignocellulosic matrix limits aqueous recovery of intracellular oil bodies. This study developed an extraction strategy combining ultrasound pretreatment with aqueous enzymatic hydrolysis using a pectinolytic cocktail (E1) and Alcalase® in simultaneous (SIM) or sequential (SEQ) configurations. Ultrasound pre-treatment markedly intensified the process, increasing oil recovery up to ~17–18% within 4 h, compared to 5–6% obtained with enzymatic treatments alone. Kinetic modelling showed configuration-dependent mechanisms: SIM and US + SIM followed pseudo-first-order kinetics, with apparent rate constants of 0.332 ± 0.007 and 0.799 ± 0.011 h^{-1}, respectively, whereas SEQ was best described by a Gompertz model ($k = 1.71 \pm 0.12\ h^{-1}$; $t_0 = 2.64 \pm 0.04$ h) and US + SEQ by a logistic model ($k = 5.72 \pm 0.45\ h^{-1}$; $t_0 = 2.36 \pm 0.04$ h). The process also enabled co-recovery of protein and carbohydrate fractions (8.03% and 8.15% respectively) under US + SEQ. The extracted oils retained a grape seed oil-like fatty acid profile dominated by linoleic acid, while US + SIM showed the strongest antioxidant activity, with IC_{50} values of 40.21 ± 0.25 μg mL^{-1} for DPPH and 29.39 ± 1.41 μg mL^{-1} for ABTS. The protein-rich fraction showed dose-dependent antimicrobial activity against *Escherichia coli*, *Pseudomonas aeruginosa*, and *Staphylococcus epidermidis*. Overall, this strategy provides a solvent-reduced route for grape seed fractionation, although key factors such as enzyme cost, ultrasound energy consumption, and downstream processing operations should be evaluated to unlock industrial scale implementation.

1. Introduction

The global cultivation of *Vitis vinifera* is one of the most economically and culturally important agricultural activities worldwide (Mussagy et al., 2026). The global vineyard surface exceeds 7 million hectares, with Europe representing the main production area (Lopes et al., 2025). In 2024, global wine production reached approximately 226 million hectolitres, with Italy, France, and Spain among the leading producers (Voccia et al., 2025). However, the wine sector generates large amounts of agro-industrial by-products that require sustainable management strategies (Chen et al., 2020; Di Fraia et al., 2024; Petrillo et al., 2021; Spigno et al., 2017).

Grape pomace, mainly composed of skins, stems, and seeds, accounts for about 20–30% of the processed grape mass (Ivanov & Godjevargova, 2024). Its disposal may cause environmental concerns due to acidic pH, high organic load, and phenolic content, contributing to soil acidification and increased Biological Oxygen Demand (BOD) and Chemical Oxygen Demand (COD) if not properly managed (Ivanov & Godjevargova, 2024; Lopes De Menezes et al., 2018; Munsch et al., 2024). Therefore, winery by-product valorisation has become increasingly relevant within circular economy and waste-to-resource approaches (Pasqualone et al., 2014; Troilo et al., 2022).

Among pomace fractions, grape seeds represent approximately 25% of the biomass and are particularly valuable due to their content of polyunsaturated fatty acids, mainly linoleic acid, tocopherols, phytosterols, proteins, dietary fibres, and phenolic compounds (Guaita et al., 2026). These features make them attractive for food, nutraceutical, cosmetic, and bioenergy applications (Samy et al., 2025; Thirumalaivasan, Nangan, et al., 2025; Yilmaz et al., 2019). Nevertheless, efficient oil extraction remains challenging because lipids are

* Corresponding author.
E-mail address: fiogabri@unina.it (G. Fiorentino).

https://doi.org/10.1016/j.fbio.2026.109748
Received 11 May 2026; Received in revised form 13 August 2026; Accepted 14 August 2026
Available online 14 August 2026
2212-4292/© 2026 The Authors. Published by Elsevier Ltd. This is an open access article under the CC BY license (http://creativecommons.org/licenses/by/4.0/).

stored in intracellular oil bodies within cotyledon cells, stabilized by phospholipids, oleosins, and a protein–polysaccharide matrix (Thirumalaivasan, Kanagaraj, et al., 2025). This structure requires extraction strategies able to disrupt both cell walls and lipid–protein assemblies.

Conventional solvent-based extraction is still widely used because of its high efficiency, but it involves large solvent volumes, high energy demand, and long processing times. Moreover, it mainly targets oil recovery, leaving other valuable fractions underexploited (Breniaux et al., 2025; Martins et al., 2023). Green technologies, including ultrasound-assisted extraction and supercritical fluid extraction, have been proposed to improve mass transfer and reduce solvent use (Breniaux et al., 2025; Thirumalaivasan, Kanagaraj, et al., 2025; Villacís-Chiriboga et al., 2026). However, these methods are often optimized for selected compounds rather than for the integrated valorisation of the whole biomass.

In this context, aqueous enzymatic extraction (AEE) has gained attention as a sustainable biorefinery strategy. Enzymes can promote the disruption of cell-wall components and protein–lipid structures under mild conditions, enabling oil recovery together with protein- and carbohydrate-rich fractions (Prezioso et al., 2026; Sun et al., 2022; Tociu et al., 2021). However, AEE efficiency strongly depends on process configuration and substrate accessibility. To the best of our knowledge, systematic comparisons between sequential and simultaneous enzymatic strategies under ultrasound-assisted conditions in highly lignified seed matrices, combined with kinetic analysis of the extraction behaviour, remain limited (Angioletti Decker et al., 2026; Ghosh et al., 2026; Matei et al., 2026; Verma et al., 2026).

Therefore, the present study aims to develop and evaluate a solvent free, ultrasound-assisted enzymatic extraction strategy for grape seeds recovered after grape marc distillation; this biomass represents a real industrial residue generated during ethanol production. The proposed approach combines physical pre-treatments with both simultaneous and sequential enzymatic hydrolysis. The objectives are: (i) to optimize oil recovery under mild, solvent-free conditions; (ii) to characterize the fatty acid composition and nutritional quality of the extracted oil; (iii) to evaluate the co-recovery of protein and carbohydrate fractions; and (iv) to assess the functional properties of the recovered products.

Overall, this work proposes a solvent free extraction strategy that enhances both yield and multi-fraction valorisation, contributing to the development of green approaches for winery by-products.

2. Materials and methods

2.1. Chemicals and reagents

All chemicals and reagents used in this study were of analytical or HPLC grade and were used as received without further purification. Bidistilled water was used for all aqueous solutions. Two commercial enzymatic formulations were employed: a pectolytic enzyme cocktail (Prezioso et al., 2026) and the protease Alcalase® (Sigma-Aldrich, Milan, Italy), as described below. Cellulase from *Trichoderma reesei* (Celluclast®, Sigma-Aldrich) and Viscozyme®-based preparations (Sigma Aldrich) were also tested.

2.2. Enzymatic cocktails

2.2.1. Pectolytic enzyme cocktail

The pectolytic cocktail (E1), kindly provided by Enolife srl (Montemesola, Italy), contained pectin lyase, pectin methylesterase, and polygalacturonase, with declared minimum activities of 50 U g^{-1}, 350 U g^{-1}, and 1750 U g^{-1}, respectively. Enzymatic activities were expressed in International Units (U), defined as the amount of enzyme capable of releasing 1 μmol of reaction product per minute under specified assay conditions.

In addition to its pectinolytic activity, E1 exhibited hydrolytic activity toward other plant cell wall polysaccharides, including xylan, carboxymethylcellulose, glucan, galactomannan, and arabinogalactan, as previously demonstrated (Prezioso et al., 2026).

2.2.2. Proteolytic enzyme (Alcalase®)

Alcalase® is a commercial protease preparation derived from *Bacillus licheniformis*, commonly used in food and bioprocessing applications. It acts primarily as an endoprotease and exhibits optimal activity in the pH range 7.0–8.5. The preparation used in this study had a declared activity of $\geq$ 0.75 Anson Units (AU) mL^{-1}. One Anson Unit corresponds to the amount of enzyme required to release 1 μmol of tyrosine equivalents per minute from casein under defined assay conditions.

2.3. Sample preparation and matrix pre-treatment

Grape seeds were supplied by Distilleria De Luca s. r.l. (Novoli, Italy) as by-products of grape marc distillation. As provided by the supplier, after distillation, the exhausted grape marc is dried in a rotary drum dryer reaching temperatures of approximately 98–100 °C; subsequently the seeds are separated from the marc and typically shipped to oil companies for extraction with organic solvents. Therefore, the recovered seeds should be considered as a pre-processed industrial by-product rather than as fresh grape seed material.

Seeds were washed with bidistilled water at room temperature for 48 h under constant agitation, to remove residual must components and free sugars that could interfere with enzymatic hydrolysis and analytical determinations; subsequently they were treated with 96% (v/v) ethanol for 20 min to detach residual sugars and surface phenolic compounds and reduce possible surface microbial contamination. Importantly, this step was intended solely for washing purposes and was not designed to extract lipids as for conventional solvent-based extraction methods. After rinsing with bidistilled water, seeds were dried in a ventilated oven at 30 °C until constant weight. Dried grape seeds were grounded using a laboratory blender (Oster, model 867-66, Auburn, Michigan, United States) and sieved to obtain a particle size $\leq$ 1.0 mm. Prior to enzymatic extraction, ground seeds were suspended in sterile bidistilled water at a solid-to-liquid (S/L) ratio of 1:6 (w/v) and subjected to a short thermal treatment at 100 °C for 5 min. This step was applied as a mild physical disruption pre-treatment to enhance cell wall permeability while minimizing thermal degradation of sensitive compounds. Samples were immediately cooled in an ice bath before further processing.

2.4. Ultrasound-assisted extraction (UAE)

Ultrasound-assisted pretreatment was performed using an ultrasonic bath (Elmasonic P, Elma Schmidbauer GmbH, Singen, Germany) operating at a frequency of 37 kHz (nominal power 130 W) and equipped with a 100 W auxiliary heating system to control the temperature raising.

Grape seed suspensions were prepared by mixing 7 g of grape seed flour with 42 mL of distilled water in 50 mL polypropylene centrifuge tubes. The tubes were positioned vertically in the central region of the bath and processed in batches. To ensure reproducibility across runs, the number of tubes, sample mass, liquid volume, and positioning configuration were kept constant for all ultrasound-assisted treatments.

The samples were sonicated for 60 min at 30 °C. Based on the nominal bath power, the specific energy input was calculated as approximately 1.60 kJ g^{-1} of suspension. This value represents a calculated process descriptor and not the actual acoustic energy delivered to each individual sample.

Non-sonicated controls were prepared as described above, but without ultrasound exposure. During the corresponding pretreatment period, the control suspensions were maintained under mechanical agitation. Following treatment, both sonicated and non-sonicated suspensions were centrifuged at 8500 × g for 15 min to separate the recovered fractions. The selected operating conditions were based on

ultrasound-assisted extraction protocols previously reported for oilseed matrices (Thilakarathna et al., 2023).

2.5. Selection of commercial enzyme cocktails and reaction conditions optimization

A preliminary screening was conducted to identify the most effective enzyme cocktails and operating conditions for oil release from grape seeds. Carbohydrase-based formulations, including Celluclast®, Viscozyme®-based preparations, and the pectolytic enzyme cocktail E1, were tested alone and in combination with Alcalase®. Enzyme loading was selected on a mass basis rather than normalized on enzymatic activity units, because the commercial preparations have different enzymatic specificities and declared activities. Solid-to-liquid (S/L) ratio and enzyme-to-substrate (E/S) ratio were preliminarily evaluated under controlled extraction conditions. The screening showed that oil recovery increased when the S/L ratio was changed from 1:4 to 1:6, whereas no relevant improvement was observed at higher ratios. Similarly, lower enzyme dosages markedly reduced oil recovery, while higher enzyme loading did not provide a proportional increase in yield. Therefore, the S/L ratio was fixed at 1:6 (w/v), and the final enzyme dosages were set at 0.1% (w/w) for the pectolytic enzyme cocktail E1 and 0.05% (w/w) for Alcalase®, both calculated with respect to dry grape seed flour mass. These conditions were selected as practical operating parameters balancing extraction efficiency and enzyme consumption.

At the selected dosage of 0.1% (w/w), E1 supplied approximately 0.050 U g^{-1} dry seed of pectin lyase, 0.350 U g^{-1} dry seed of pectin methylesterase, and 1.750 U g^{-1} dry seed of polygalacturonase, based on the supplier-declared minimum activities. Alcalase® had a declared activity of ≥0.75 Anson Units (AU) mL^{-1} and a density of 1.18 g mL^{-1} at 20 °C. Therefore, at the selected dosage of 0.05% (w/w), Alcalase® supplied approximately $\geq 3.2 \times 10^{-4}$ AU g^{-1} dry seed.

Oil extraction was monitored after 0, 0.5, 1, 2, 3, 4, 6, 8, 12, 18, and 24 h of incubation with the enzyme mixtures. Since oil yield reached a plateau after approximately 4–6 h, an extraction time of 4 h was selected as the standard condition for subsequent experiments.

2.6. Enzyme treatment

Enzyme treatment of grape seeds was carried out in 50 mM sodium citrate buffer (pH 5.0) under mild agitation (120 rpm), following two different protocols:(i) a simultaneous enzymatic treatment (SIM), in which E1 (0.1% w/w) and Alcalase® (0.05% w/w) were added at the beginning of the reaction, and the suspension was incubated at 40 °C for 4 h; (ii) a sequential enzymatic treatment (SEQ), in which E1 (0.1% w/w) was first added and incubated at 37 °C for 2 h at pH 5.0; then the pH was adjusted to 6.5 by dropwise addition of 0.5 M $NaHCO_3$ solution followed by the addition of Alcalase® (0.05% w/w) and further incubation for 2 h at 55 °C. Combined treatments included ultrasound pretreatment prior to enzymatic hydrolysis. After the enzymatic incubation, samples were centrifuged at 8500 × g for 15 min at 30 °C, resulting in separation into an oil layer (grape seed oil, GSO) and a protein–lipid emulsion (grape seed protein, GSP), and a solid residual phase (press cake). After oil yield determination, the recovered oil was immediately analysed for fatty acid composition and FTIR characterization. Conversely, the protein-rich cream and the carbohydrate-rich aqueous fractions, were frozen stored in sealed containers at −20 °C until compositional, FTIR, and antimicrobial analyses.

2.7. Oil yield determination and pH monitoring

Oil yield was determined gravimetrically and expressed as a percentage relative to the initial dry mass of grape seeds:

$$\text{Oil yield (\%)} = \frac{\text{mass of extracted oil}}{\text{initial mass of grape seeds}} \times 100$$

The pH of the reaction slurry was monitored at defined time intervals (0, 0.5, 1, 2, 3, 4, 6, 8, 12, 18, and 24 h) using a calibrated pH electrode in order to determine changes in the pH of the biomass during the enzymatic hydrolysis step.

2.7.1. Kinetic modelling of oil extraction

Oil extraction kinetic data were fitted by nonlinear regression using three kinetic models: pseudo-first-order, Gompertz, and logistic models (Polmann et al., 2019). The pseudo-first-order model was used to describe extraction profiles characterized by a progressive approach to an asymptotic yield and was expressed as:

$$Y(t) = Y\infty[1 - exp(-kt)]$$

where Y(t) is the oil yield at extraction time t, Y∞ is the asymptotic oil yield predicted by the model, and k is the apparent extraction rate constant.

Sigmoidal extraction profiles were described using Gompertz and logistic models. The Gompertz model was expressed as:

$$Y(t) = Y\infty exp\{ - exp[- k(t - t_0)]\}$$

where Y∞ is the maximum predicted oil yield, k is the apparent slope parameter, and t_0 is the inflection time.

The logistic model was expressed as:

$$Y(t) = \frac{Y\infty}{\{1 + exp[- k(t - t_0)]\}}$$

where Y∞ is the maximum predicted oil yield, k is the logistic slope parameter, and t_0 is the inflection time.

Model adequacy was evaluated using R^2, adjusted R^2 (R^2adj), RMSE, corrected Akaike Information Criterion (AICc), and residual analysis. Adjusted R^2 was used to account for the different number of fitted parameters among the tested models, while RMSE was used to quantify the average prediction error. Residual plots were inspected to verify the absence of evident systematic trends and to support model selection beyond R^2 values alone.

2.8. Fatty acid composition

The analysed matrices were treated for 15 min at 60 °C with a 10% boron trifluoride/methanol solution (1.4 M, 0.8 mL) and 100 μL of dimethoxy propane (Di Meo, Salzano, et al., 2023). Before lipid extraction, a known amount of heptadecanoic acid (C17:0) was added as an internal standard. The internal standard was carried through all analytical steps, including extraction, transmethylation, and GC–FID analysis, to correct for analytical variability and ensure reliable quantification of fatty acid methyl esters. Then, each solution was extracted twice with *n*-hexane, and the organic phases were combined and dried. The resulting fatty acid methyl esters were redissolved in *n*-hexane, filtered through a Millex filter, and injected into a gas chromatograph (Di Meo, Giacco, et al., 2023). The gas chromatography (GC) apparatus consisted of an Agilent GC 8890 A instrument equipped with a split/splitless injector and flame ionization detector (FID detector, and an Agilent 7693 A automatic liquid sampler. The analysis was performed using an Agilent HP-88 capillary column (100 m × 0.25 mm, film thickness 0.20 μm). The following parameters were set during the experiments: sample volume injected, 0.8 mL, fed into the injector via an autosampler heated to 250 °C, with a split ratio of 100:1; N_2 carrier gas, 40 psi, constant pressure mode; oven heating program: 100 °C (10 min), 10 °C min^{-1} to 180 °C (5 min), 1 °C min^{-1} to 200 °C (25 min), 4 °C min^{-1} to 230 °C (10 min); detector temperature: 280 °C; H_2: 40 mL min^{-1}; air: 400 mL min^{-1}; compensation gas: 25 mL min^{-1}. Fatty acid methyl esters were identified by comparing their retention times with those of 22 commercial fatty acid standards purchased from Supelco (Sigma-Aldrich Group, St. Louis, MO, USA), with the limit of

quantitation of 14 ppb. Representative GC–FID chromatograms of the fatty acid methyl esters obtained from SIM, SEQ, US + SIM, and US + SEQ oil samples are reported in the Supplementary Material as Fig. S3A–D.

2.9. Calculated oxidizability index

The calculated oxidizability value (COX) was determined according to Fatemi and Hammond (Fatemi & Hammond, 1980):

$$\mathrm{COX} = \frac{1(C16:1 + C17:1 + C18:1 + C20:1) + 10.3(C18:2) + 21.6(C18:3 + C20:3)}{100}$$

2.10. Nutritional quality indices

Lipid quality indices were calculated from fatty acid composition using the following equations (Ulbricht & Southgate, 1991):

Atherogenicity Index (AI)

$$AI = \frac{C12:0 + 4C14:0 + C16:0}{\sum MUFA + \sum \omega 6 + \sum \omega 3}$$

Thrombogenicity index (TI) (Santos-Silva et al., 2002)

$$TI = \frac{C14:0 + C16:0 + C18:0}{0.5\sum MUFA + 0.5\sum \omega 6 + 3\sum \omega 3 + (\omega 3/\omega 6)}$$

Hypocholesterolemic/Hypercholesterolemic ratio (HH) (Martínez-Pineda et al., 2024)

$$HH = \frac{C18:1 + C18:2 + C18:3 + C20:4 + C20:5 + C22:5 + C22:6}{C14:0 + C16:0}$$

2.11. Antioxidant activity of grape seed oil extracts

2.11.1. DPPH• radical scavenging assay

The DPPH• radical scavenging activity of grape seed oil extracts was determined according to (Pérez et al., 2015). Briefly, 50 μL of each extract, prepared at concentrations of 12.5, 25, 50, 100, and 200 μg mL^{-1}, were mixed with 150 μL of DPPH• ethanolic solution, 400 μM, in a 96-well microplate. The reaction mixture was incubated for 30 min at 37 °C in the dark, and the absorbance was then measured at 517 nm using a microplate reader.

DPPH• radical scavenging activity was expressed as percentage inhibition and calculated as follows:

$$\textit{DPPH scavenging activity}\ (\%) = \frac{(A_{control} - A_{sample})}{A_{control}} x\ 100$$

where A control is the absorbance of the DPPH• solution without sample, and A sample is the absorbance of the reaction mixture containing the grape seed oil extract.

2.11.2. ABTS•$^+$ radical scavenging assay

The ABTS•$^+$ radical scavenging activity was evaluated using the ABTS radical cation decolorization assay, according to Perez et al. with minor modifications (Pérez et al., 2015). The ABTS•$^+$ radical cation was generated by reacting 7 mM ABTS aqueous solution with $K_2S_2O_8$, at a final concentration of 2.45 mM. The mixture was kept in the dark at room temperature for 12–16 h. Before use, the ABTS•$^+$ solution was diluted with ethanol to an absorbance of 0.700 ± 0.020 at 734 nm.

For the assay, 190 μL of diluted ABTS•$^+$ solution was mixed with 10 μL of grape seed oil extract, prepared at concentrations ranging from 12.5 to 200 μg mL^{-1}, in a final volume of 200 μL. After 6 min of reaction at room temperature, the absorbance was measured at 734 nm using a microplate reader.

ABTS•$^+$ radical scavenging activity was expressed as percentage inhibition and calculated as follows:

$$\textit{ABTS scavenging activity}\ (\%) = \frac{(A_{control} - A_{sample})}{A_{control}} x\ 100$$

where A control is the absorbance of the ABTS•$^+$ solution without sample, and A sample is the absorbance measured in the presence of the grape seed oil extract.

2.11.3. IC_{50} determination

The antioxidant efficiency of grape seed oil extracts was further assessed by calculating the IC_{50} values for both DPPH• and ABTS•$^+$ assays. IC_{50} was defined as the extract concentration required to achieve 50% radical scavenging activity.

IC_{50} values were obtained from concentration–response curves built using the inhibition values measured at 12.5, 25, 50, 100, and 200 μg mL^{-1}. The curves were fitted by nonlinear regression analysis. Lower IC_{50} values were considered indicative of higher antioxidant activity. IC_{50} values were calculated for each independent replicate and expressed as mean ± standard deviation.

2.12. Protein quantification

The dried material was weighed and analysed for protein content using the Bradford colorimetric assay and Bovine serum albumin (BSA) as the standard (Kruger, 2009). for protein concentration estimation. Bovine serum albumin (BSA) was used as the standard for protein concentration estimation. Protein concentration was expressed as a percentage (% w/w) relative to the freeze-dried mass. To enable comparison with oil recovery, the protein yield was calculated as the amount of protein recovered relative to the initial dry mass of grape seeds, according to the following equation:

$$\text{Protein yield}\ (\%) = \frac{\text{mass of protein in the recovered fraction}\ (g)}{\text{initial dry mass of grape seeds}\ (g)} \times 100$$

The mass of protein in the recovered fraction was obtained by multiplying the protein concentration (% w/w) by the total mass of the freeze-dried fraction. The contribution of externally added enzymes (E1 and Alcalase®) was accounted for and subtracted from the total protein content, to estimate only the protein fraction derived from grape seeds.

2.13. Carbohydrate determination

Total carbohydrate content in the aqueous phase was determined using a sulfuric acid-based colorimetric method (Albalasmeh et al., 2013). Briefly, 1 mL of sample was mixed with 3 mL of concentrated sulfuric acid and vortexed for 30 s. After rapid heating, the mixture was cooled in ice for 2 min before measuring A315nm. Absorbance was then measured at 315 nm using a UV spectrophotometer. Blanks were prepared using deionized water. Quantification was performed using a glucose calibration curve. To enable comparison among different extraction conditions, the carbohydrate yield was calculated as the amount of carbohydrates recovered in the aqueous phase relative to the initial dry mass of grape seeds, according to the following equation:

$$\text{Carbohydrate yield (\%)} = \frac{\text{mass of carbohydrates in aqueous phase (g)}}{\text{initial dry mass of grape seeds (g)}} \times 100$$

2.14. FTIR analysis

Fourier Transform Infrared (FTIR) spectroscopy was performed on GSO, GSP, and press cake. Spectra were recorded over the range of 4000–600 cm^{-1} with a resolution of 4 cm^{-1}. FTIR spectroscopy was conducted using a PerkinElmer GX spectrometer. KBr pellets were prepared by mixing 3 mg of dried sample (either oil, protein, or biomass residue) with 197 mg of KBr. For oil analysis, a drop of oil was deposited onto the KBr pellet surface. For protein and biomass samples, lyophilized powdered material was used. FTIR spectra were recorded and processed using Origin software (v.2022b, OriginLab Corporation, Northampton, MA, USA).

2.15. Antimicrobial activity

Antimicrobial activity of GSO and GSP was assessed by the agar disk diffusion method against *Staphylococcus epidermidis*, *Pseudomonas aeruginosa*, and *Escherichia coli*. Bacterial strains were cultured in Luria–Bertani (LB) broth at 37 °C for 18 h. The cultures were then adjusted to a density corresponding to ~ 1.0×10^8 CFU mL^{-1}, and 100 μL of the suspension were evenly spread onto LB agar plates. Grape seed oil samples were diluted in dimethyl sulfoxide (DMSO, 50% v/v) prior to application. Protein fractions were dissolved in sterile distilled water and applied to sterile paper disks to reach amounts of 10, 15, and 20 μg per disk. The disks were placed onto the inoculated agar surface and plates were incubated at 37 °C for 18–24 h.

Antimicrobial activity was determined by measuring the diameter of the inhibition zones (mm). Vancomycin (for *S. epidermidis*) and Polymyxin B (for *P. aeruginosa* and *E. coli*) were used as positive controls at equivalent amounts. Sterile LB broth and distilled water served as negative controls for protein fractions, while DMSO and LB broth were used as solvent controls for oil samples. All experiments were performed in triplicate, and results were expressed as mean inhibition zone diameter (mm).

2.16. Statistical analysis

All experiments were performed in three independent biological replicates, each measured in technical triplicate. Results are reported as mean ± SD of the biological replicates (n = 3). Statistical analyses were performed using GraphPad Prism 10. One-way analysis of variance (ANOVA) followed by Tukey's multiple comparison test was used to compare oil yield, protein recovery, carbohydrate recovery, fatty acid composition, lipid quality indices and IC_{50} values among the different extraction treatments. Antioxidant activity data obtained from DPPH• and $ABTS^{\bullet+}$ radical scavenging assays were analysed by two-way ANOVA, considering extraction treatment and sample concentration as fixed factors, followed by Tukey's multiple comparison test. Multiple comparisons were performed among treatments within each concentration. IC_{50} values were calculated for each independent replicate from nonlinear regression of the concentration-response curves and were then compared among treatments by one-way ANOVA followed by Tukey's HSD test. Antimicrobial data were analysed by two-way ANOVA followed by Tukey's multiple comparison test. Differences were considered statistically significant at $p < 0.05$.

Kinetic data were fitted by nonlinear regression using pseudo-first-order, Gompertz, and logistic models. Model adequacy was evaluated using R^2, corrected Akaike Information Criterion (AICc), RMSE, and residual analysis. AICc was calculated using the same number of experimental time points for each treatment (n = 11). The pseudo-first-order model was treated as a two-parameter model (Y∞, k), whereas Gompertz and logistic models were treated as three-parameter models (Y∞, k, t_0). Residual plots were inspected to verify the absence of evident systematic trends and to support model selection beyond R^2 values alone.

3. Results and discussion

3.1. Optimization to recover oil and high value bioactive compounds

This study aimed to valorise grape seed biomass through the selective recovery of oil and high value bioactive compounds within a green extraction framework. In this context, preliminary experiments were carried out to develop and optimize an AEE protocol for oil recovery from grape seeds derived from grape marc distillation, and to evaluate the effect of an additional UAE pre-treatment. A preliminary screening of different commercial enzymatic preparations was performed to identify the most suitable system for promoting oil release under aqueous conditions. The tested formulations included a pectinolytic cocktail (E1), a cellulolytic/hemicellulolytic preparation (Viscozyme®), cellulase from *T. reesei* (Celluclast®), and the proteolytic enzyme mixture Alcalase®. In all the preliminary experiments, oil yield was adopted as the key response variable.

The use of carbohydrase-based preparations alone resulted in negligible oil recovery. Specifically, the pectinolytic cocktail E1 led to oil yields below 1.3%, while Viscozyme® resulted in yields below 1.1%. Similarly, treatment with Celluclast® did not produce detectable oil extraction recovery. The use of Alcalase® alone also resulted in low yields (<0.9%). These results indicate that neither polysaccharide degradation nor proteolysis, when acting individually, are sufficient to effectively disrupt the lipid–protein matrix entrapping oil bodies in grape seed biomass.

Therefore, the combined action of cell wall degrading enzymes and proteases was investigated, with the aim of targeting both the structural polysaccharides of the cell wall and the proteinaceous components associated with oleosomes. Enzymes were tested in both simultaneous (SIM) and sequential (SEQ) configurations, and the reaction conditions for each approach were optimized.

Among all the combinations tested, the E1–Alcalase® system demonstrated the highest efficiency compared with the Celluclast® + Alacalase® and Viscozyme® + Alcalase® combinations. Interestingly,

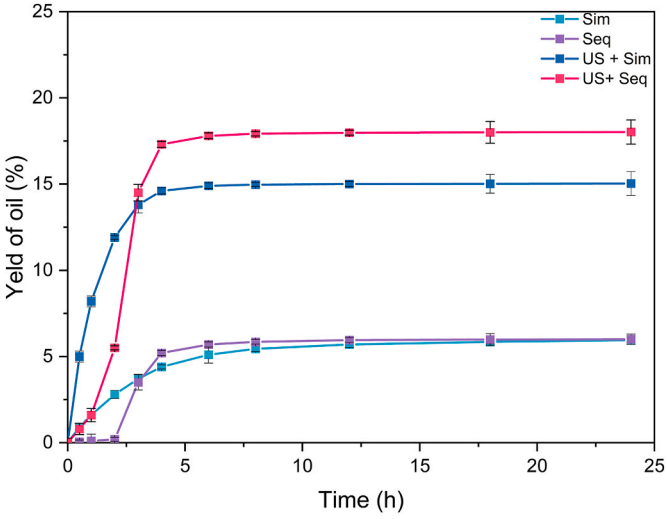


Fig. 1. Time-dependent oil yield (%) obtained under simultaneous (SIM), sequential (SEQ), ultrasound-assisted simultaneous (US + SIM), and ultrasound-assisted sequential (US + SEQ) enzymatic treatments. Data are expressed as mean ± standard deviation of three independent extraction experiments (n = 3).

E1 contains a combination of pectin-degrading enzymes, including pectin lyase, pectin methylesterase, and polygalacturonase, together with additional side activities toward hemicellulosic and non-pectic polysaccharides, such as xylan, glucan, galactomannan, and arabinogalactan (Prezioso et al., 2026).

The E1–Alcalase® system was therefore selected for subsequent optimization. Grape seeds were incubated for 4 h with the addition of different enzyme cocktails in either sequential or simultaneous mode. The simultaneous configuration (SIM) yielded approximately 5.0% oil, while the sequential protocol (SEQ) reached 5.3%, corresponding to a four-to five-fold increase compared with the individual enzyme treatments (Fig. 1). In contrast, the treatment with Viscozyme® + Alcalase® resulted in yields below 3.8%, whereas Celluclast® + Alcalase® achieved only 1.3%, highlighting the limited efficacy of these enzyme systems.

The superior performance of the E1–Alcalase® system may be attributed to the complementary action of a multifunctional carbohydrase preparation and a proteolytic enzyme. E1 may promote cell-wall disruption, increase matrix porosity and improving access to the embedded oil bodies, while Alcalase® may hydrolyse oleosome-associated proteins and destabilise lipid–protein structures, thereby facilitating oil release. After identifying E1 and Alcalase® as the most effective enzyme combination, the main process parameters, including enzyme dosage and solid-to-liquid ratio (S/L) were further evaluated. Enzyme dosages of 0.1% (w/w) for E1 and 0.05% (w/w) for Alcalase® were found to be optimal. This optimal ratio may reflect the complementary role of Alcalase®, whose proteolytic activity supports the matrix-degrading action of E1 by hydrolysing proteinaceous structures associated with oil bodies. At the same time, limited the Alcalase® dosage may prevent excessive proteolysis, particularly under simultaneous treatment conditions, where high protease concentrations could partially degrade the proteinaceous components of the E1 cocktail and reduce the synergistic effect between the two enzymes.

Regarding, the solid-to-liquid (S/L) ratio, 1:6 (w/v) was determined as optimal. Ratios lower than 1:6 (w/v) caused biomass aggregation and limited enzyme accessibility, whereas higher dilution ratios reduced oil recovery because of inefficient droplet coalescence and phase separation.

Overall, these results demonstrate that both enzyme synergy and careful optimization of process parameters are essential to achieve effective matrix disruption and efficient oil recovery. To further intensify the extraction process, UAE was introduced as a mild physical strategy prior to the optimized enzymatic treatment. With the aim of enhancing matrix disruption and mass transfer, thereby improving enzyme accessibility and oil release.

The effect of UAE was evaluated by comparing the time-dependent oil extraction profiles obtained under simultaneous (SIM), sequential (SEQ) enzyme treatment, UAE + SIM, and UAE + SEQ conditions (Fig. 1).

In the absence of UAE, both SIM and SEQ protocols exhibited relatively slow extraction kinetics and lower final oil recoveries. The SIM treatment showed a gradual and asymptotic increase in oil yield, reaching ~ 5.95% after 24 h and approaching a plateau after 6–8 h.

However, from a process perspective, the increase in oil yield beyond 4 h was minimal, indicating that most of the extractable oil had already been released within this time frame. Therefore, although the theoretical plateau was reached at longer times (4–6 h), 4 h was considered a practical equilibrium time, ensuring a favourable balance between extraction efficiency and process duration.

The SEQ protocol achieved a comparable final yield (≈6.00%) but displayed a pronounced initial lag phase (0–2 h), indicating that preliminary structural modifications were required before effective oil release could occur. The introduction of ultrasound significantly intensified and accelerated the process. Under UAE + SIM conditions, oil yield reached ~ 5.0% within the first 30 min, nearly matching the final yield obtained after 24 h under non-sonicated conditions. The final oil recovery increased to ~ 15.0%, corresponding to a ~2.5-fold enhancement compared with SIM (Fig. 1). The highest performance was observed under UAE + SEQ conditions, where oil recovery reached ≈18.0%. Notably, about 96% of the total oil was extracted within the first 4 h (≈17.3%), with only marginal increases thereafter. These results demonstrate that the combination of ultrasound-induced structural disruption and sequential enzymatic hydrolysis significantly enhances matrix permeability and accelerates mass transfer, leading to faster and more efficient oil recovery.

Our results are particularly relevant when compared with the literature. Traditional AEE of oilseeds typically requires between 12 and 24 h to achieve significant oil yields (Goula et al., 2018; Torabizadeh & Khaki, 2025). In contrast, in the present system, the integration of ultrasound enabled the extraction equilibrium to be reached within only 4 h, corresponding to an ~ 80% reduction in processing time.

3.2. Kinetic modelling and mechanistic interpretation

To quantitatively describe the extraction dynamics, the experimental data were fitted using pseudo-first-order, Gompertz, and logistic kinetic models; the results fitted curves and kinetic parameters are shown in Fig. S1 and Table 1, respectively. Model selection was based on the combined evaluation of AICc, adjusted R^2, RMSE, and residual distribution.

As shown in Table 1, the pseudo-first-order model provided the best fit for SIM and US + SIM, showing the lowest AICc and RMSE values and supporting a diffusion-controlled extraction behaviour. In contrast, SEQ was better described by the Gompertz model, while US + SEQ was best fitted by the logistic model, consistently with the sigmoidal extraction profiles observed experimentally. Residual plots did not show evident systematic trends, further supporting the suitability of the selected models for describing the different extraction behaviours (Fig. S2). For the SIM and US + SIM the constant under ultrasound-assisted conditions suggests that ultrasound pretreatment reduced mass-transfer limitations, thereby promoting faster oil release.

In contrast, the kinetic profile observed for the SEQ treatment showed a sigmoidal behaviour and was best described by the Gompertz model, highlighting the presence of an initial induction phase preceding rapid oil release. This trend suggests that a preliminary stage of matrix weakening is required before efficient proteolytic disruption of oleosome-associated proteins can take place.

The US + SEQ condition was instead best described by the logistic model, which accurately captured the characteristic inflection point observed at ~ 2.4–2.6 h. The higher kinetic constant obtained under these conditions indicates that matrix degradation proceeds more rapidly once a critical threshold of structural disintegration is reached.

Overall, these results suggest distinct extraction mechanisms among the tested treatments. Simultaneous treatments appear to be mainly governed by gradual diffusion-controlled processes, whereas sequential treatments may involve a more complex two-step behaviour, characterized by an initial increase in substrate accessibility followed by faster enzymatic destabilization. Ultrasound likely promotes both extraction behaviours, through cavitation-related physical effects that improve solvent penetration, enzyme accessibility, and mass transfer. However, since direct structural characterization of ultrasound-induced matrix disruption was not performed in the present study, the proposed contribution of cavitation should be interpreted as a plausible explanation rather than as direct structural evidence. In addition to the extraction strategy, the physicochemical characteristics of the raw material may also have contributed to the observed extraction kinetics. The thermal history of the grape seeds, including both industrial high-temperature drying and the additional short thermal pretreatment applied in this study, could have modified matrix porosity and enzyme accessibility. Nevertheless, the oil yields obtained indicate that adequate enzyme–substrate accessibility was retained under all the tested conditions.

Table 1
Kinetic model fitting statistics for oil extraction under simultaneous enzymatic treatment (SIM), sequential enzymatic treatment (SEQ), ultrasound-assisted simultaneous treatment (US + SIM), and ultrasound-assisted sequential treatment (US + SEQ). The best-supported model for each treatment was selected based on the lowest corrected Akaike Information Criterion (AICc), together with a high adjusted coefficient of determination (R^2adj), a low root mean square error (RMSE), and an appropriate residual distribution. The check mark indicates the selected best-fit model.

Treatment	Model	Y∞ (g/100 g)	R^2	R^2adj	RMSE	AICc	Best fit
SIM	Pseudo-first-order	5.888	0.9995	0.9994	0.046	−62.11	✓
	Gompertz	5.730	0.9908	0.9869	0.196	−26.44	
	Logistic	5.651	0.9796	0.9709	0.292	−17.69	
SEQ	Pseudo-first-order	6.405	0.8754	0.8442	0.942	+4.18	
	Gompertz	5.884	0.9987	0.9981	0.096	−42.18	✓
	Logistic	5.833	0.9960	0.9943	0.169	−29.69	
US + SIM	Pseudo-first-order	15.048	0.9997	0.9996	0.079	−50.36	✓
	Gompertz	14.831	0.9882	0.9831	0.528	−4.62	
	Logistic	14.730	0.9744	0.9634	0.779	+3.94	
US + SEQ	Pseudo-first-order	18.921	0.9140	0.8925	2.220	+23.04	
	Gompertz	17.971	0.9950	0.9929	0.533	−4.40	
	Logistic	17.960	0.9988	0.9983	0.260	−20.21	✓

Note. Y∞ = asymptotic maximum oil yield, expressed as g oil/100 g dry matter; R^2adj = adjusted coefficient of determination; RMSE = root mean square error; AICc = corrected Akaike Information Criterion.

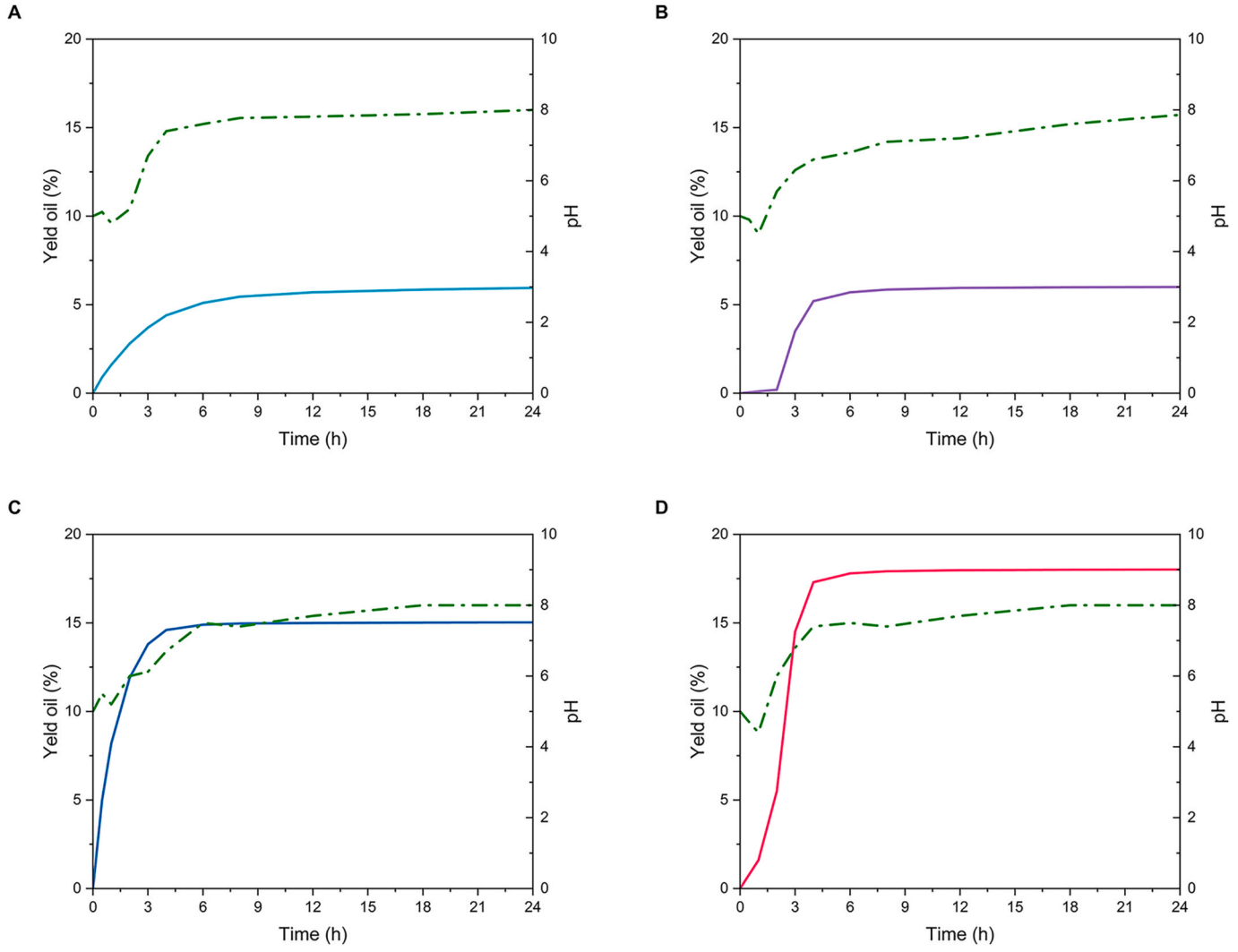


Fig. 2. Coupled evolution of oil yield and pH during enzyme-assisted aqueous extraction of grape seed oil under (A) simultaneous enzymatic treatment (SIM), (B) sequential enzymatic treatment (SEQ), (C) ultrasound-assisted simultaneous treatment (US + SIM), and (D) ultrasound-assisted sequential treatment (US + SEQ). Oil yield is plotted on the left y-axis and represented by solid-coloured lines, whereas pH is plotted on the right y-axis and represented by dashed green lines. Data are presented as mean ± standard deviation (n = 3).

3.3. Combined analysis of pH evolution and reaction kinetics

To gain deeper insight into the mechanisms governing oil release, extraction kinetics were analysed together with pH evolution during the process (Fig. 2). In AEE systems, oil release depends on the progressive disruption of two main structural barriers: the plant cell wall and the oil body interface, which regulate matrix permeability and accessibility of entrapped compounds (Gao et al., 2024; Vovk et al., 2023). The pH changes observed during extraction likely reflected the combined effects of enzymatic hydrolysis, matrix solubilisation, and the buffering capacity of grape-seed components. In Alcalase®-containing treatments, proteolysis generated soluble peptides and new terminal amino and carboxyl groups, altering the proton balance of the medium. Since no pH-stat control was applied, the observed pH drift should be interpreted as the net effect of these processes. Although some free fatty acid release may have occurred, the upward pH trend was more consistent with proteolysis and protein solubilisation. The progressive shift towards less acidic conditions may also have favoured Alcalase® activity, as this protease is active under neutral-to-alkaline conditions. This could have enhanced the disruption of proteinaceous structures associated with cell walls, oil bodies and intercellular matrix structures, thereby promoting oil release during the initial extraction stages (Rosenthal et al., 1996; Wu et al., 2009).

Altogether, the pH profile is consistent with the hypothesis that proteolysis contributed to progressive matrix deconstruction, thereby facilitating oil release.

3.4. Fractionation, recovery, and characterization of biomass components

To evaluate the efficiency of the different extraction strategies, the recovery of oil, proteins, and carbohydrates was compared after 4 h of extraction, corresponding to the process-relevant equilibrium time under UAE conditions (Fig. 3).

As discussed above, oil recovery was strongly influenced by the extraction protocol, with ultrasound-assisted treatments significantly improving lipid extraction up to 17%. This result is consistent with previous studies on AEE and ultrasound-assisted approaches for oilseed processing (Chen et al., 2020; Goula et al., 2018; Villacís-Chiriboga et al., 2026).

A similar enhancement pattern was observed for protein recovery (Fig. 3). Conventional treatments resulted in limited extraction, with average recoveries of 1.20% for SIM and 1.97% for SEQ, whereas ultrasound-assisted conditions increased protein recovery to 6.00% in US + SIM and 8.03% in US + SEQ. The highest recovery obtained under US + SEQ suggests that the combination of ultrasound and sequential enzymatic hydrolysis effectively promotes protein release (Salzano et al., 2024). Comparable effects have been described in plant-based systems and fibre-rich oat side streams where ultrasound-assisted enzymatic treatments enhance enzyme accessibility and protein release (Villacís-Chiriboga et al., 2026; Wang et al., 2023).

Carbohydrate recovery was also influenced by the extraction strategy. The average carbohydrate recoveries were 6.45% for SIM and 4.65% for SEQ, whereas ultrasound-assisted conditions increased recoveries to 8.25% (US + SIM) and 8.15% (US + SEQ). These results indicate that ultrasound also plays a key role also in promoting the release of soluble carbohydrates. In contrast to proteins, carbohydrate recovery was only slightly influenced by the enzymatic sequence once ultrasound was applied, suggesting that ultrasound-driven matrix disruption itself is the dominant role in factor governing polysaccharide release (Ebringerová & Hromádková, 2010; Le Guillard et al., 2016; Sharma et al., 2025). This interpretation is consistent with previous findings on the extraction of hydrophilic components from plant biomass (Ferraioli et al., 2025).

Overall, these results demonstrate that ultrasound-assisted enzymatic extraction enables the simultaneous recovery of both lipophilic and hydrophilic fractions under mild conditions, without the use of organic solvents during the extraction step, thus highlighting the potential of this approach for future integrated biorefinery strategies targeting grape seed valorisation.

Compared with the literature, the present system shows improved process performance: while conventional AEE of oilseeds typically requires 12–24 h to achieve significant yields, the integration of ultrasound allowed equilibrium to be reached within 4 h, corresponding to an ~ 80% reduction in processing time (Ebringerová & Hromádková, 2010). The addition of ultrasound further enhances extraction efficiency and may improve oil quality parameters, such as oxidative stability (Ivetić et al., 2017; Maria et al., 2026; Mohapatra & Singh, 2026).

More broadly, the integration of enzymatic and ultrasound-assisted extraction strategies represents a promising approach for the valorisation of agro-industrial residues within future biorefinery concepts. In

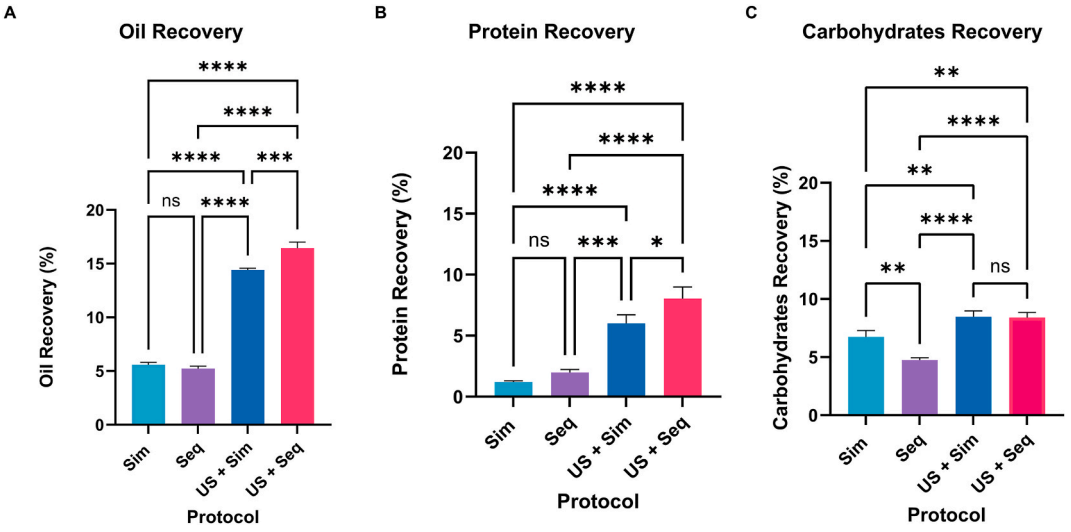


Fig. 3. Recovery of (a) oil, (b) proteins, and (c) carbohydrates obtained after 4 h of extraction under different treatment conditions: simultaneous enzymatic treatment (SIM), sequential enzymatic treatment (SEQ), ultrasound-assisted simultaneous treatment (US + SIM), and ultrasound-assisted sequential treatment (US + SEQ). Data are presented as mean ± standard deviation of three independent extraction experiments (n = 3). Statistical differences among treatments were evaluated separately for each recovered fraction by one-way ANOVA followed by Tukey's multiple comparison test. Statistical significance is indicated as *p < 0.05, **p < 0.01, ***p < 0.001, ****p < 0.0001; ns = not significant.

Table 2
Main fatty acids identified in grape seed oil under different extraction conditions. Results are expressed as percentages of total fatty acids and values are reported as the mean ± SD (n = 3). Different lowercase superscript letters within the same row indicate statistically significant differences among extraction treatments according to one-way ANOVA followed by Tukey's post hoc test ($p < 0.05$). Values sharing the same letter are not significantly different.

Fatty Acid	SIM	SEQ	US + SIM	US + SEQ
Linoleic (18:2 n-6)	69.32 ± 0.55^{b}	65.01 ± 0.30^{c}	72.86 ± 0.20^{a}	68.68 ± 0.55^{b}
Oleic (18:1 n-9)	18.79 ± 0.22^{a}	19.25 ± 0.81^{a}	14.77 ± 0.85^{c}	16.69 ± 0.12^{b}
Palmitic (16:0)	8.28 ± 0.10^{b}	11.26 ± 0.19^{a}	8.42 ± 0.15^{b}	11.21 ± 0.87^{a}
Stearic (18:0)	2.58 ± 0.25^{b}	3.28 ± 0.05^{a}	3.05 ± 0.09^{a}	2.23 ± 0.05^{b}
Palmitoleic (16:1)	0.07 ± 0.001^{c}	0.02 ± 0.001^{d}	0.09 ± 0.002^{b}	0.11 ± 0.001^{a}

this context, the US + SEQ protocol enables the recovery of multiple valuable streams, including lipids, proteins, and soluble carbohydrates, from industrially generated grape seeds through a single aqueous extraction process, highlighting its potential for the valorisation of winemaking residues.

3.5. *Influence of extraction protocols on the fatty acid profile of recovered grape seed oil fractions*

The fatty acid composition of the lipid fractions recovered under the different extraction conditions was compared to evaluate whether the extraction strategy influenced oil composition quality in addition to recovery yield. As reported in Table 2, all extraction treatments yielded oils with comparable fatty acid profiles, indicating that neither ultrasound pretreatment nor the different enzymatic extraction strategies substantially altered lipid composition. Linoleic acid was the predominant fatty acid, followed by oleic, palmitic, and stearic acids, in agreement with the characteristic fatty acid profile of grape seed oil (Dimić et al., 2020; Zhao et al., 2019).

Although the general fatty acid pattern was conserved among treatments, differences were observed in the relative abundance of individual fatty acids and fatty acid classes. It should be considered that fatty acid data are expressed as relative percentages of total fatty acids; therefore, variations may reflect differences in the relative recovery of specific lipid fractions rather than actual modifications of lipid composition. Overall, 22 fatty acids were identified across the analysed samples, including saturated (SFA), monounsaturated (MUFA), and polyunsaturated fatty acids (PUFA), with the major components reported in Table 2.

Linoleic acid content ranged from 65.01% in SEQ to 72.86% in US + SIM, confirming the predominance of ω-6 PUFA in grape seed oil. Conversely, oleic acid showed higher relative abundance in SIM and SEQ, whereas lower values were observed in ultrasound-assisted treatments, particularly US + SIM. Palmitic acid exhibited higher levels in SEQ and US + SEQ, while lower relative amounts were detected in SIM and US + SIM. The fatty acid class distribution further supported the influence of extraction conditions on the relative selectivity of lipid recovery, as reported in Table 3.

The grape seeds used in this study were recovered from industrial grape marc processing and had therefore undergone thermal exposure during distillation. However, thermal treatment is also an inherent step in conventional grape seed oil production, where industrial drying prior to solvent extraction may involve temperatures close to 98–100 °C (Akterian et al., 2025). Therefore, differences in fatty acid composition compared with literature data cannot be attributed exclusively to the previous thermal exposure but should also be interpreted considering the intrinsic variability associated with grape cultivar, geographical origin, environmental conditions, and processing practices.

Taken together, these results indicate that the extraction protocols did not induce major alterations in the intrinsic fatty acid profile of grape seed oil but rather affected the relative recovery of lipid fractions. In particular, SIM, especially when combined with ultrasound, appeared to favour the recovery of a more PUFA-enriched fraction, whereas SEQ tended to result in a relatively higher contribution of MUFA/ω-9 fatty acids. The simultaneous action of carbohydrases and proteases may have promoted a more extensive disruption of the seed matrix, facilitating the release of a broader lipid fraction, whereas the sequential enzymatic strategy may have favoured a more selective extraction following an ordered degradation of structural components. Ultrasound pretreatment may have further enhanced these effects by improving matrix disruption and enzyme accessibility, in agreement with previous studies on ultrasound- and enzyme-assisted extraction of oil-rich plant matrices (Laqui-Estaña et al., 2024; Lezama Guerra et al., 2025; Passos et al., 2009).

The fatty acid composition was further evaluated through the calculated oxidizability value and lipid nutritional quality indices, namely COX, AI, TI, and HH, as shown in Table 4.

COX values suggest that treatments favouring PUFA recovery may also increase the theoretical susceptibility of the oil to oxidation.

The nutritional quality indices confirmed an overall favourable lipid profile for all recovered oil fractions. AI and TI values were low across all

Table 3
Fatty acid class distribution of grape seed oil obtained under different extraction conditions. Results are expressed as percentages of total fatty acids and are reported as the mean ± standard deviation of three independent experiments (n = 3). Different lowercase superscript letters within the same row indicate statistically significant differences among extraction treatments according to one-way ANOVA followed by Tukey's post hoc test ($p < 0.05$). Values sharing the same letter are not significantly different. The SFA/MUFA ratio was calculated to evaluate the balance between saturated and monounsaturated fatty acid fractions.

	SIM	SEQ	US + SIM	US + SEQ
SFA (%)	10.90 ± 0.32^{b}	14.54 ± 0.45^{a}	11.52 ± 0.28^{b}	13.44 ± 0.41^{a}
MUFA (%)	18.96 ± 0.55^{a}	19.37 ± 0.61^{a}	14.91 ± 0.38^{c}	16.84 ± 0.50^{b}
PUFA (%)	69.38 ± 1.12^{b}	65.04 ± 0.98^{c}	72.88 ± 1.05^{a}	68.70 ± 0.89^{b}
SFA/MUFA	0.57 ± 0.02^{c}	0.75 ± 0.03^{b}	0.77 ± 0.02^{b}	0.80 ± 0.03^{a}
ω-3 (%)	0.02 ± 0.005	0.03 ± 0.007	0.01 ± 0.002	0.01 ± 0.003
ω-6 (%)	70.12 ± 1.15^{b}	66.06 ± 0.95^{c}	73.57 ± 1.21^{a}	69.71 ± 0.92^{b}
ω-9 (%)	18.88 ± 0.52^{a}	19.35 ± 0.58^{a}	14.82 ± 0.35^{c}	16.73 ± 0.48^{b}

Note. SFA = saturated fatty acids; MUFA = monounsaturated fatty acids; PUFA = polyunsaturated fatty acids; ω-3, ω-6, and ω-9 = omega-3, omega-6, and omega-9 fatty acid families, respectively.

Table 4
Lipid nutritional quality and oxidative stability indices of grape seed oil obtained under different extraction conditions. Results are reported as the mean ± standard deviation (SD) of three independent experiments (n = 3). Different lowercase superscript letters within the same row indicate statistically significant differences among extraction treatments according to one-way ANOVA followed by Tukey's post hoc test ($p < 0.05$). Values sharing the same letter are not significantly different.

Index	SIM	SEQ	US + SIM	US + SEQ
COX	7.32 ± 0.15^{a}	6.91 ± 0.12^{b}	7.62 ± 0.18^{a}	7.24 ± 0.14^{ab}
AI	0.29 ± 0.01^{b}	0.44 ± 0.02^{a}	0.30 ± 0.01^{b}	0.42 ± 0.02^{a}
TI	0.66 ± 0.02^{b}	1.02 ± 0.04^{a}	0.72 ± 0.02^{b}	0.95 ± 0.03^{a}
HH	8.10 ± 0.25^{a}	5.80 ± 0.18^{b}	7.60 ± 0.22^{a}	6.30 ± 0.19^{b}

Note. COX = calculated oxidizability value; AI = atherogenicity index; TI = thrombogenicity index; HH = hypocholesterolemic/hypercholesterolemic ratio.

samples, with the most favourable values observed for SIM and US + SIM. These treatments also showed the highest HH ratios, indicating a greater relative contribution of hypocholesterolemic fatty acids. Conversely, SEQ and US + SEQ showed higher AI and TI values and lower HH ratios, in line with their higher SFA contents.

Taken together, these findings suggest that the selection of the extraction strategy influence the balance between nutritional characteristics and oxidative stability of grape seed oil recovered from industrial winemaking residues. SIM-based treatments appear more favourable in terms of fatty acid-related nutritional indices, likely due to the higher relative contribution of PUFA, whereas SEQ resulted in fractions with lower calculated oxidizability values, reflecting a relatively higher contribution of more oxidation-resistant fatty acids. Therefore, the extraction protocol should be selected according to the target application, considering not only oil yield but also the compositional and stability-related characteristics of the recovered lipid fraction.

3.6. Antioxidant activity of grape seed oils obtained under different extraction conditions

To complement the information provided by lipid quality indices and the calculated oxidizability value (COX), the antioxidant activity of grape seed oils obtained under the different extraction conditions was evaluated using DPPH• and ABTS•$^{+}$ radical scavenging assays. These assays provide complementary information, as they assess the radical scavenging capacity of the recovered oils rather than their theoretical susceptibility to oxidation.

Both DPPH• and ABTS•$^{+}$ assays showed a concentration-dependent increase in radical scavenging activity for all samples, with US + SIM generally showing the highest response and SEQ the lowest activity across the tested concentration range. SIM and US + SEQ displayed intermediate behaviour, with SIM showing slightly higher activity than US + SEQ at the highest concentration (Fig. 4A and B).

Two-way ANOVA confirmed that both extraction protocol and concentration significantly affected radical scavenging activity, with significant differences among treatments within each concentration. Moreover, under all tested conditions, the ABTS•$^{+}$ assay showed higher radical scavenging responses than the DPPH• assay, suggesting a greater sensitivity toward the antioxidant-active compounds present in the recovered grape seed oils, as also previously reported (Pérez et al., 2015). The antioxidant efficiency of the oils was further evaluated through IC_{50} determination, defined as the concentration required to achieve 50% radical scavenging activity (Table 5).

Table 5
IC_{50} values of grape seed oils determined by DPPH• and ABTS•$^{+}$ radical scavenging assays under different extraction conditions. Data are expressed as the mean ± standard deviation (SD) of three independent experiments (n = 3). Different lowercase superscript letters within the same column indicate statistically significant differences among extraction treatments according to one-way ANOVA followed by Tukey's HSD test ($p < 0.05$). Values sharing the same letter are not significantly different. Lower IC_{50} values indicate higher antioxidant activity.

	IC_{50} DPPH (μg mL^{-1})	IC_{50} ABTS (μg mL^{-1})
US + SIM	40.21 ± 0.25 ^{c}	29.39 ± 1.41 ^{c}
SIM	50.33 ± 0.61 ^{b}	38.10 ± 1.84 ^{b}
US + SEQ	53.01 ± 0.95 ^{b}	37.58 ± 2.20 ^{b}
SEQ	79.95 ± 0.95 ^{a}	58.74 ± 2.65 ^{a}

While the fatty acid profile remained largely conserved among treatments, antioxidant-related parameters showed greater variability, likely reflecting the different selectivity of each protocol in recovering antioxidant-active compounds from the grape seed matrix. Compared with major lipid components, antioxidant-active compounds are often more sensitive to extraction conditions, as their recovery and apparent activity can depend on matrix accessibility, extraction parameters, and interactions with the surrounding matrix. In the present study, the observed differences refer exclusively to the overall radical-scavenging activity of the recovered extracts rather than to changes in the abundance of specific antioxidant molecules.

This interpretation is also relevant when comparing antioxidant activity with COX values. Although lipid fractions enriched in polyunsaturated fatty acids may display higher calculated oxidizability and therefore greater theoretical susceptibility to oxidation, they may also exhibit higher radical scavenging activity when extraction conditions favour the recovery of antioxidant-active minor compounds. Accordingly, lipid quality indices, COX values, and antioxidant assays should be considered complementary descriptors of oil quality.

Overall, these results suggest that ultrasound-assisted simultaneous enzymatic treatment favours the recovery of antioxidant-active compounds from grape seed biomass, as indicated by the higher radical scavenging activity observed among the tested conditions. Further studies are therefore required to identify and quantify the specific antioxidant-active compounds responsible for this activity, in order to better clarify the relationship between extraction conditions, oil composition, and antioxidant potential.

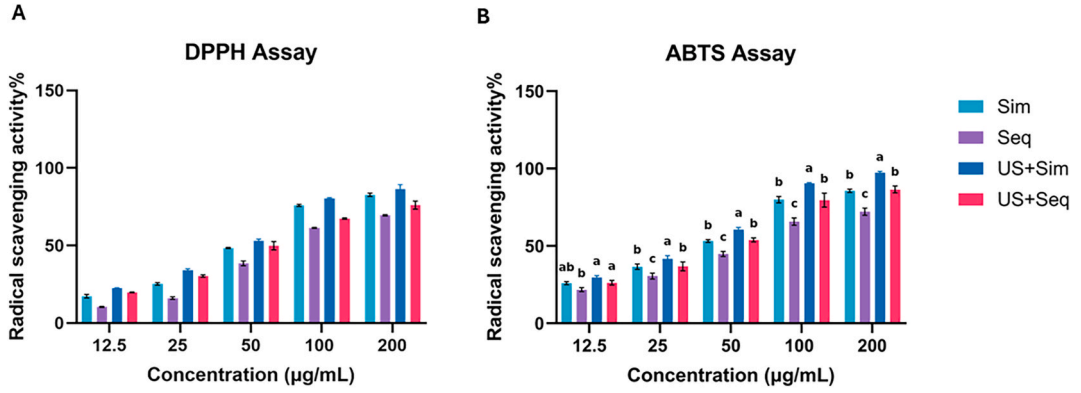


Fig. 4. Antioxidant activity of grape seed oils obtained under different extraction conditions. Radical scavenging activity was determined using the DPPH• assay (A) and ABTS•$^{+}$ assay (B) at concentrations ranging from 12.5 to 200 μg mL^{-1} for SIM, SEQ, US + SIM, and US + SEQ samples. Data are expressed as the mean ± standard deviation (SD) of three independent experiments (n = 3). Statistical differences among extraction treatments were evaluated within each concentration by two-way ANOVA followed by Tukey's multiple-comparison test. Different letters above the bars indicate statistically significant differences among treatments at the same concentration ($p < 0.05$).

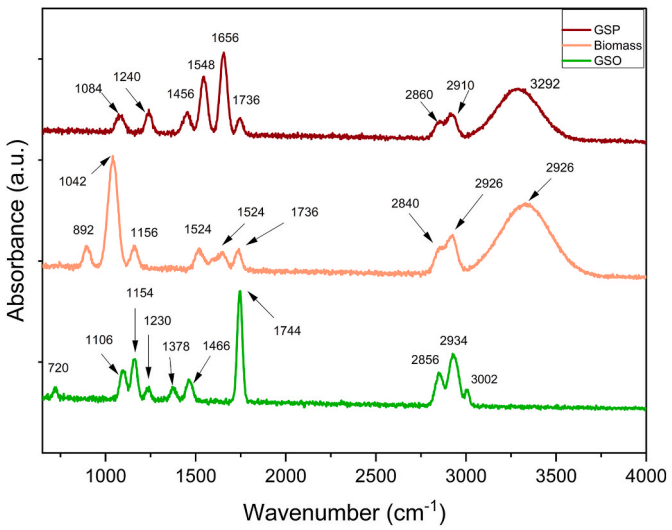


Fig. 5. FTIR spectra of grape seed-derived fractions, including oil, biomass residue, and cream fraction. Spectra are reported in the range 4000–650 cm^{-1} and presented as absorbance (a.u.) versus wavenumber (cm^{-1}).

3.7. Characterization of functional groups in the extracted fractions using FTIR analysis

To evaluate the efficiency of the US + SEQ protocol and assess the chemical integrity of the extracted products, Fourier-transform infrared spectroscopy (FTIR) was performed on the recovered oil, the protein-rich cream fraction, and the residual biomass (Fig. 5). The FTIR spectrum of the oil fraction exhibited the characteristic absorption bands of triglyceride-rich vegetable oils. A strong band at ~ 1744 cm^{-1} was observed, corresponding to the stretching vibration of ester carbonyl groups (C=O), which is a distinctive feature of triacylglycerols. Additional intense bands at 2926 and 2856 cm^{-1} were assigned to the asymmetric and symmetric stretching vibrations of aliphatic CH_2 groups, respectively, associated with long hydrocarbon chains of fatty acids. A weaker peak around 3002 cm^{-1} was also detected and attributed to = CH stretching vibrations, indicating the presence of unsaturated fatty acids.

The FTIR spectrum of the cream fraction displayed a more complex profile, reflecting the coexistence of lipids and proteins within this intermediate phase. In particular, the bands at 1656 and 1548 cm^{-1} correspond to Amide I and Amide II vibrations, respectively, characteristic of protein structures (De Meutter & Goormaghtigh, 2021; López-Lorente & Mizaikoff, 2016) likely originating from partially hydrolysed cellular structures and protein–lipid complexes released during enzymatic treatment. Additionally, a band around 1736 cm^{-1} indicates the presence of lipid components, suggesting that the cream fraction represents an emulsion-like system composed of both proteins and lipids (Pancholi et al., 2023). To further support the interpretation of the proteinaceous character of the GSP fraction, the Amide I region was qualitatively deconvoluted in the 1700–1600 cm^{-1} range. The baseline-corrected spectrum, total fitted curve, individual Gaussian components, and fitting details are reported in the Supplementary Material as Fig. S4, while the corresponding peak positions, relative areas, and tentative secondary-structure assignments are summarized in Table S2. The fitted components were tentatively assigned to β-sheet/aggregated structures, random coil or unordered structures, α-helical contributions, β-turns, and high-wavenumber β-sheet β-sheet/aggregated structures, according to literature-reported Amide I sub-band regions.

The FTIR spectrum of the residual biomass showed prominent absorption bands in the 1000–1200 cm^{-1} region, particularly at ~ 1042 and 1156 cm^{-1}, which are associated with C–O stretching vibrations of polysaccharides such as cellulose and hemicellulose (Jiang et al., 2025). These signals confirm the presence of carbohydrate-rich structural components remaining in the solid matrix after extraction. Additional bands near 2926 cm^{-1} were also observed and attributed to aliphatic CH stretching vibrations, likely arising from residual lipids or structural organic components (Mašán et al., 2021).

Overall, FTIR analysis confirmed the successful fractionation of industrial grape seed biomass into chemically distinguishable fractions enriched in lipid, protein, and carbohydrate components. These findings complement the compositional and functional analyses, supporting the potential of the proposed strategy for the integrated valorisation of grape seed residues.

3.8. Antimicrobial activity of grape seed-derived fractions

To support the integrated valorisation of grape seed biomass, the optimized extraction process was complemented by an assessment of the antimicrobial potential of the recovered fractions. The antimicrobial activity of grape seed-derived protein and oil fractions was evaluated against *E. coli*, *P. aeruginosa*, and *S. epidermidis* using agar disc diffusion assays (Fig. 6). Representative images of the agar diffusion plates obtained for the antimicrobial assays are reported in the Supplementary Material as Fig. S5.

Both grape seed-derived fractions exhibited dose-dependent antimicrobial activity, although the extent of inhibition varied depending on the fraction and bacterial strain (Fig. 6). Overall, the protein-rich fraction showed greater antimicrobial effectiveness than the oil fraction, while the antibiotic control showed the highest inhibitory activity under all tested conditions. Against *E. coli*, the protein-rich fraction produced inhibition zones of approximately 10–17 mm, compared with 5–10 mm for the oil fraction. A similar trend was observed against *P. aeruginosa*, although with lower overall susceptibility, with inhibition zones ranging from approximately 9–17 mm for the protein-rich fraction and 4–7 mm for the oil fraction. Conversely, *S. epidermidis* showed higher sensitivity, with inhibition zones of approximately 10–15 mm for the protein-rich fraction and 7–12 mm for the oil fraction. Statistical analysis confirmed significant differences among fractions and experimental conditions.

The higher antimicrobial activity of the protein-rich fraction may be associated with the presence of bioactive peptides generated during enzymatic hydrolysis. Antimicrobial peptides derived from plant protein hydrolysates have been widely described, and their activity is commonly related to interactions with bacterial membranes, leading to increased permeability and loss of membrane integrity. For example, Alcalase-derived cowpea protein hydrolysates showed antibacterial activity against both Gram-negative and Gram-positive bacteria, including *E. coli* and *P. aeruginosa* (Osman et al., 2021) and plant protein hydrolysates are increasingly recognised as promising sources of antimicrobial peptides (Rivero-Pino et al., 2023). However, since peptide identification and membrane-integrity analyses were not performed in the present study, this mechanism should be considered a plausible interpretation rather than direct evidence. Further molecular characterization will be required to identify the active components and establish possible structure–activity relationships.

The antimicrobial activity observed for the protein-rich fraction was comparable with values reported for grape seed extracts. Zhu et al. (2015), for instance, reported an inhibition zone of 14.8 ± 0.21 mm against *E. coli* O157 using 3.2 mg of grape seed extract per disc. In the present study, similar inhibition levels were obtained using lower amounts of the protein fraction. However, direct comparisons among disc-diffusion studies should be interpreted cautiously because antimicrobial responses are strongly influenced by extract composition, solvent or dispersion system, bacterial strain, compound diffusivity, and assay conditions. Moreover, since the protein-rich fraction was recovered from an industrially processed feedstock, the possible influence of upstream processing on protein integrity and biological activity cannot

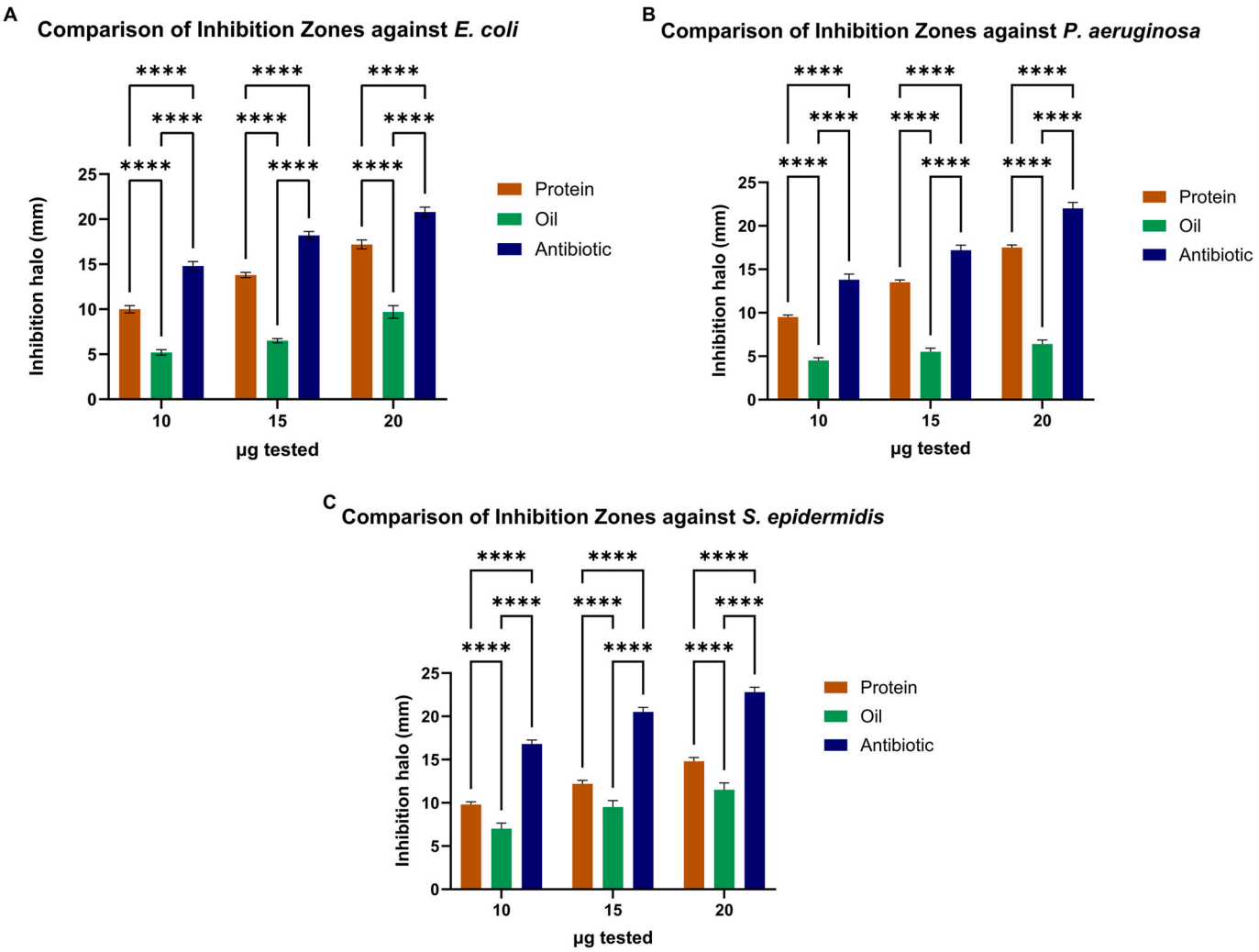


Fig. 6. Antimicrobial activity of grape seed-derived protein and oil fractions.
Antimicrobial activity of grape seed-derived fractions evaluated by inhibition disc halo diffusion assay against *E. coli*, *P. aeruginosa*, and *S. epidermidis*. The inhibition zones (mm) are reported for the protein fraction (brown), oil fraction (green), and antibiotic control (blue) at increasing concentrations (10, 15, and 20 µg). Data are presented as mean ± standard deviation (n = 3). Statistical significance was assessed by two-way ANOVA followed by Tukey's multiple comparison multiple-comparison test; **** indicates $p < 0.0001$.

be excluded.

The lower susceptibility of *P. aeruginosa* is consistent with its well-established intrinsic resistance, which is associated with low outer-membrane permeability and efficient efflux systems (Li et al., 1994). Therefore, the measurable inhibition observed for this strain is noteworthy and supports further investigation using quantitative antimicrobial assays, including minimum inhibitory concentration (MIC) and minimum bactericidal concentration (MBC) determinations.

The oil fraction also displayed measurable antimicrobial activity, although its effect was consistently lower than that of the protein-rich fraction. This effect may be related to the presence of unsaturated fatty acids, particularly linoleic acid, which have been reported to interfere with bacterial membrane integrity and lipid metabolism (Parsons et al., 2012; Zheng et al., 2005). The greater susceptibility of the Gram-positive strain *S. epidermidis* compared with the Gram-negative bacteria is consistent with this interpretation. However, because the diffusion of hydrophobic compounds in agar is limited and depends strongly on the dispersion system, the antimicrobial potential of the oil fraction should be confirmed using broth-based assays.

Overall, these findings show that the ultrasound-assisted enzymatic extraction strategy enabled the recovery of both an oil fraction and a protein-rich fraction with measurable antimicrobial activity, supporting the integrated valorisation of industrial grape seed residues. Further studies will be required to characterize the active compounds, determine MIC and MBC values, and assess process-related factors, including water consumption, enzyme dosage, energy demand, pretreatment requirements, and downstream processing, within future larger-scale application.

4. Conclusions

This study demonstrates that grape seed biomass can be valorised through an integrated ultrasound-assisted enzymatic extraction strategy, enabling the recovery of multiple fractions with distinct composition and functionality. Compared with conventional approaches, the combined use of ultrasound and enzymes enhanced lipid recovery under mild aqueous conditions, suggesting that process intensification may improve matrix accessibility and mass transfer. Kinetic modelling revealed a strong dependence of extraction behaviour on treatment configuration, with ultrasound-assisted processes reaching higher yields and faster release rates, while sequential and simultaneous enzymatic strategies followed distinct extraction patterns reflecting differences in matrix accessibility and substrate hydrolysis.

Beyond extraction performance, the recovered fractions showed

differentiated functional properties that contribute to the overall value of the process. The lipid fraction retained the characteristic fatty acid profile of grape seed oil and exhibited measurable radical scavenging activity, supporting its potential as a functional oil stream. In contrast, the protein-rich fraction displayed significant antimicrobial activity against *E. coli*, *P. aeruginosa*, and *S. epidermidis*, likely associated with peptide species generated during enzymatic hydrolysis. These findings highlight the importance of considering not only extraction yield, but also the functional properties of the recovered fractions.

Overall, the results support the feasibility of an ultrasound-assisted enzymatic approach for the fractionation of grape seed biomass under mild conditions, enabling the simultaneous recovery of oil, antioxidants, and protein-rich fractions with added functionality. The proposed strategy reduces the need for organic solvents and shows potential for improving extraction performance compared with conventional approaches. This work highlights the potential of grape seed biomass as a multifunctional raw material for the development of value-added ingredients and supports resource-efficient strategies for the valorisation of agro-industrial residues. However, further studies, including techno-economic assessment, life cycle analysis, and pilot-scale validation, are required to fully evaluate its industrial applicability.

Abbreviation	Meaning
ABTS•$^+$	2,2′-azino-bis(3-ethylbenzothiazoline-6-sulphonic acid) radical cation
AEE	Aqueous Enzymatic Extraction
AI	Atherogenicity Index
AICc	Corrected Akaike Information Criterion
ANOVA	Analysis of Variance
AU	Anson Units
BOD	Biological Oxygen Demand
BSA	Bovine Serum Albumin
CFU	Colony-Forming Units
COD	Chemical Oxygen Demand
COX value	Calculated Oxidizability Value
DMSO	Dimethyl Sulfoxide
DPPH•	1,1-diphenyl-2-picrylhydrazyl radical
E/S	Enzyme-to-Substrate Ratio
E1	Pectinolytic Enzyme Cocktail
FAO	Food and Agriculture Organization
FID	Flame Ionization Detector
FTIR	Fourier Transform Infrared Spectroscopy
GC	Gas Chromatography
GSO	Grape Seed Oil
GSP	Grape Seed Protein
HH	Hypocholesterolemic/Hypercholesterolemic Ratio
IC_{50}	Half-Maximal Inhibitory Concentration
KBr	Potassium Bromide
LB	Luria-Bertani
MUFA	Monounsaturated Fatty Acids
PUFA	Polyunsaturated Fatty Acids
R^2	Coefficient of Determination
R^2adj	Adjusted Coefficient of Determination
RMSE	Root Mean Square Error
SD	Standard Deviation
SEQ	Sequential Enzymatic Treatment
SIM	Simultaneous Enzymatic Treatment
S/L	Solid-to-Liquid Ratio
SFA	Saturated Fatty Acids
SFE	Supercritical Fluid Extraction
SWE	Subcritical Water Extraction
TI	Thrombogenicity Index
U	Enzymatic Unit
UAE	Ultrasound-Assisted Extraction
US + SEQ	Ultrasound-Assisted Sequential Enzymatic Treatment
US + SIM	Ultrasound-Assisted Simultaneous Enzymatic Treatment
UV	Ultraviolet
Y∞	Asymptotic Maximum Yield
k	Apparent Extraction Rate Constant or Slope Parameter
t_0	Inflection Time
ω-3	Omega-3 Fatty Acids
ω-6	Omega-6 Fatty Acids
ω-9	Omega-9 Fatty Acids

CRediT authorship contribution statement

Alessia Di Fraia: Conceptualization, Data curation, Formal analysis, Methodology, Software, Writing – original draft, Writing – review & editing. **Martina Aulitto:** Data curation, Writing – review & editing. **Danila Limauro:** Data curation, Writing – review & editing. **Vito Michele Paradiso:** Conceptualization, Data curation, Writing – review & editing. **Armando Zarrelli:** Data curation, Formal analysis, Methodology, Writing – review & editing. **Gabriella Fiorentino:** Conceptualization, Data curation, Formal analysis, Funding acquisition, Supervision, Writing – original draft, Writing – review & editing.

Declaration of generative AI and AI-assisted technologies

During the preparation of this work, AI-assisted tools were used for the graphical refinement of the graphical abstract. The authors carefully reviewed and edited the final version and take full responsibility for the content of the published article.

Declaration of competing interests

The authors declare that they have no competing financial interests or personal relationships that could have influenced the work reported in this paper.

Acknowledgements

This work was supported by the Italian Ministry of University and Research (MUR) under the PRIN 2022 funding program AGRI_FOOD CHIP (E53C24003120006).

Appendix A. Supplementary data

Supplementary data to this article can be found online at https://doi.org/10.1016/j.fbio.2026.109748.

Data availability

Data will be made available on request.

References

Akterian, S., Fikiin, K., Georgiev, G., & Terziev, A. (2025). Pre-treatment equipment for processing grape marc into valorised by-products: A review. *Sustainability, 17*(13), 6188. https://doi.org/10.3390/su17136188

Albalasmeh, A. A., Berhe, A. A., & Ghezzehei, T. A. (2013). A new method for rapid determination of carbohydrate and total carbon concentrations using UV spectrophotometry. *Carbohydrate Polymers, 97*(2), 253–261. https://doi.org/10.1016/j.carbpol.2013.04.072

Angioletti Decker, B. L., Fonteles, T. V., Fernandes, F. A. N., & Rodrigues, S. (2026). Green extraction technologies for valorising Brazilian agri-food waste. *Sustainable Food Technology, 4*(1), 62–88. https://doi.org/10.1039/D5FB00323G

Breniaux, M., Poulain, B., Mariño-Cortegoso, S., Barbosa-Pereira, L., Nioi, C., & Ghidossi, R. (2025). Valorization of grape seed By-Products using subcritical water extraction: A sustainable approach for bioactive compound recovery. *Processes, 13*(6), 1788. https://doi.org/10.3390/pr13061788

Chen, Y., Wen, J., Deng, Z., Pan, X., Xie, X., & Peng, C. (2020). Effective utilization of food wastes: Bioactivity of grape seed extraction and its application in food industry. *Journal of Functional Foods, 73*, Article 104113. https://doi.org/10.1016/j.jff.2020.104113

De Meutter, J., & Goormaghtigh, E. (2021). Amino acid side chain contribution to protein FTIR spectra: Impact on secondary structure evaluation. *European Biophysics Journal, 50*(3–4), 641–651. https://doi.org/10.1007/s00249-021-01507-7

Di Fraia, S., Di Meglio, A., Massarotti, N., Vanoli, L., Bentivoglio, R., & Volpecina, V. (2024). Energy recovery and waste valorization in a frozen food processing facility: A case study from Lazio, Italy. *Energy Efficiency, 17*(3), 13. https://doi.org/10.1007/s12053-024-10193-1

Di Meo, M. C., Giacco, A., Zarrelli, A., Mandrone, V. M., D'Angelo, L., Silvestri, E., De Girolamo, P., & Varricchio, E. (2023). Effects of Olea europaea L. polyphenols on the animal welfare and milk quality in dairy cows. *Animals, 13*(20), 3225. https://doi.org/10.3390/ani13203225

Di Meo, M. C., Salzano, A., Zotti, T., Palladino, A., Giaquinto, D., Maruccio, L., Romanucci, R., Rocco, M., Zarrelli, A., D'Occhio, M. J., Campanile, G., &

Varricchio, E. (2023). Plasma fatty acid profile in Italian Holstein-Friesian dairy cows supplemented with natural polyphenols from the olive plant Olea Europaea L. *Veterinary and Animal Science, 21*, Article 100298. https://doi.org/10.1016/j.vas.2023.100298

Dimić, I., Teslić, N., Putnik, P., Bursać Kovačević, D., Zeković, Z., Šojić, B., Mrkonjić, Ž., Čolović, D., Montesano, D., & Pavlić, B. (2020). Innovative and conventional valorizations of grape seeds from winery By-Products as sustainable source of lipophilic antioxidants. *Antioxidants, 9*(7), 568. https://doi.org/10.3390/antiox9070568

Ebringerová, A., & Hromádková, Z. (2010). An overview on the application of ultrasound in extraction, separation and purification of plant polysaccharides. *Central European Journal of Chemistry, 8*(2), 243–257. https://doi.org/10.2478/s11532-010-0006-2

Fatemi, S. H., & Hammond, E. G. (1980). Analysis of oleate, linoleate and linolenate hydroperoxides in oxidized ester mixtures. *Lipids, 15*(5), 379–385. https://doi.org/10.1007/BF02533555

Ferraioli, A., Miele, N. A., Di Pierro, P., & Cavella, S. (2025). Enzymatic extraction increases the recovery of protein and antioxidant compounds from wheat bran. *Lebensmittel-Wissenschaft und -Technologie, 234*, Article 118575. https://doi.org/10.1016/j.lwt.2025.118575

Gao, Y., Ding, Z., Liu, Y., & Xu, Y.-J. (2024). Aqueous enzymatic extraction: A green, environmentally friendly and sustainable oil extraction technology. *Trends in Food Science & Technology, 144*, Article 104315. https://doi.org/10.1016/j.tifs.2023.104315

Ghosh, S., Dey, S., Sen, K., Dibra, A., Pastorino, P., Saha, N. C., & Saha, S. (2026). Case study on biorefinery products derived from food and agro-industrial wastes. In *Food and agro-industrial wastes* (pp. 399–416). Elsevier. https://doi.org/10.1016/B978-0-443-31654-8.00027-8.

Goula, A. M., Papatheodorou, A., Karasavva, S., & Kaderides, K. (2018). Ultrasound-assisted aqueous enzymatic extraction of oil from pomegranate seeds. *Waste and Biomass Valorization, 9*, 1–11. https://doi.org/10.1007/s12649-016-9740-9

Guaita, M., Zocco, A., Messina, S., Motta, S., Coisson, J. D., & Bosso, A. (2026). Polyphenolic profile and dietary fiber content of skins and seeds from unfermented and fermented grape pomace. *Molecules, 31*(5), 788. https://doi.org/10.3390/molecules31050788

Ivanov, Y., & Godjevargova, T. (2024). Antimicrobial polymer films with grape seed and skin extracts for food packaging. *Microorganisms, 12*(7), 1378. https://doi.org/10.3390/microorganisms12071378

Ivetić, D.Ž., Omorjan, R. P., Đorđević, T. R., & Antov, M. G. (2017). The impact of ultrasound pretreatment on the enzymatic hydrolysis of cellulose from sugar beet shreds: Modeling of the experimental results. *Environmental Progress & Sustainable Energy, 36*(4), 1164–1172. https://doi.org/10.1002/ep.12544

Jiang, Z., Chen, J., Guo, X., Chen, F., Guo, X., Wang, Q., & Jiao, B. (2025). Mechanism and potential of aqueous enzymatic extraction for constructing green production System for lipids and proteins. *Foods, 14*(23), 3981. https://doi.org/10.3390/foods14233981

Kruger, N. J. (2009). The Bradford method for protein quantitation. In J. M. Walker (Ed.), *The protein protocols handbook* (pp. 17–24). Humana Press. https://doi.org/10.1007/978-1-59745-198-7_4.

Laqui-Estaña, J., Obreque-Slier, E., García-Nauto, N., & Saldaña, E. (2024). Advances in grape seed oil extraction techniques and their applications in food products: A comprehensive review and bibliometric analysis. *Foods, 13*(22), 3561. https://doi.org/10.3390/foods13223561

Le Guillard, C., Bergé, J.-P., Donnay-Moreno, C., Bruzac, S., Ragon, J.-Y., Baron, R., Fleurence, J., & Dumay, J. (2016). Soft liquefaction of the red seaweed grateloupia turuturu yamada by ultrasound-assisted enzymatic hydrolysis process. *Journal of Applied Phycology, 28*(4), 2575–2585. https://doi.org/10.1007/s10811-015-0788-x

Lezama Guerra, K. S., Pascual Chagman, G. J., Brandolini, A., Hidalgo, A., Florez-Jalixto, M. A., & Encina-Zelada, C. R. (2025). Influence of cellulase pretreatment on the quality characteristics, total phenolic content, and antioxidant capacity of hydraulic press-extracted grapeseed oil. *Polish Journal of Food and Nutrition Sciences*, 375–386. https://doi.org/10.31883/pjfns/214149

Li, X. Z., Livermore, D. M., & Nikaido, H. (1994). Role of efflux pump(s) in intrinsic resistance of Pseudomonas aeruginosa: Resistance to tetracycline, chloramphenicol, and norfloxacin. *Antimicrobial Agents and Chemotherapy, 38*(8), 1732–1741. https://doi.org/10.1128/AAC.38.8.1732

Lopes, J. D. C., Madureira, J., Margaça, F. M. A., & Cabo Verde, S. (2025). Grape pomace: A review of its bioactive phenolic compounds, health benefits, and applications. *Molecules, 30*(2), 362. https://doi.org/10.3390/molecules30020362

Lopes De Menezes, M., Johann, G., Diório, A., Pereira, N. C., & Da Silva, E. A. (2018). Phenomenological determination of mass transfer parameters of oil extraction from grape biomass waste. *Journal of Cleaner Production, 176*, 130–139. https://doi.org/10.1016/j.jclepro.2017.12.128

López-Lorente, Á. I., & Mizaikoff, B. (2016). Mid-infrared spectroscopy for protein analysis: Potential and challenges. *Analytical and Bioanalytical Chemistry, 408*(11), 2875–2889. https://doi.org/10.1007/s00216-016-9375-5

Maria, L., Jorge, O., Arnulfo, A., Hoyos, N., Guerra, M., Delgado, J., & Arrazola, G. (2026). Optimization of coconut oil extraction through microwave drying and enzymatic–ultrasound treatment with emphasis on yield and quality parameters. *Discover Food, 6*(1), 108. https://doi.org/10.1007/s44187-026-00848-6

Martínez-Pineda, M., Juan, T., Antoniewska-Krzeska, A., Vercet, A., Abenoza, M., Yagüe-Ruiz, C., & Rutkowska, J. (2024). Exploring the potential of yellow mealworm (Tenebrio molitor) oil as a nutraceutical ingredient. *Foods, 13*(23), 3867. https://doi.org/10.3390/foods13233867

Martins, R., Barbosa, A., Advinha, B., Sales, H., Pontes, R., & Nunes, J. (2023). Green extraction techniques of bioactive compounds: A state-of-the-art review. *Processes, 11*(8), 2255. https://doi.org/10.3390/pr11082255

Mašán, V., Matwijczuk, A. P., Niemczynowicz, A., Kycia, R. A., Karcz, D., Gładyszewska, B., Ślusarczyk, L., & Burg, P. (2021). Chemometric approach to characterization of the selected grape seed oils based on their fatty acids composition and FTIR spectroscopy. *Scientific Reports, 11*(1), Article 19256. https://doi.org/10.1038/s41598-021-98763-6

Matei, E., Cosma, L., Râpă, M., Calotă, A.-S., Predescu, A. M., Stoica, A., & Coman, G. (2026). Valorization of agri-food waste from pigment-rich root vegetable in integrated EU Biorefinery systems. *Foods, 15*(8), 1432. https://doi.org/10.3390/foods15081432

Mohapatra, M., & Singh, S. (2026). Paradigm shift of food industry waste into high-valued resources through valorisation as an integrated sustainable approach. In S. Dey, & M. P. Shah (Eds.), *Microbial applications in industrial wastewater treatment* (pp. 275–295). Singapore: Springer Nature. https://doi.org/10.1007/978-981-96-9128-9_12.

Munsch, T., Malinowska, M. A., Unlubayir, M., Ferrier, M., Abdallah, C., Gémin, M.-P., Billet, K., & Lanoue, A. (2024). Classification of grape seed residues from distillation industries in Europe according to the polyphenol composition highlights the influence of variety, geographical origin and color. *Food Chemistry X, 22*, Article 101362. https://doi.org/10.1016/j.fochx.2024.101362

Mussagy, C. U., Caicedo-Paz, A. V., General, V. V., Cruz-Diaz, A. L., Peixoto, G., & Raghavan, V. (2026). Sequential multi-stage biorefinery of chilean Winemaking residues: Recovery of high-value compounds and environmental impact of anthocyanins on phenolic-modified anaerobic digestion for bioenergy production. *Biomass and Bioenergy, 209*, Article 109033. https://doi.org/10.1016/j.biombioe.2026.109033

Osman, A., Enan, G., Al-Mohammadi, A.-R., Abdel-Shafi, S., Abdel-Hameid, S., Sitohy, M. Z., & El-Gazzar, N. (2021). Antibacterial peptides produced by Alcalase from cowpea seed proteins. *Antibiotics, 10*(7), 870. https://doi.org/10.3390/antibiotics10070870

Pancholi, M. J., Khristi, A. M. A. K., & Bagchi, D. (2023). Comparative analysis of lignocellulose agricultural waste and pre-treatment conditions with FTIR and machine learning modeling. *BioEnergy Research, 16*(1), 123–137. https://doi.org/10.1007/s12155-022-10444-y

Parsons, J. B., Yao, J., Frank, M. W., Jackson, P., & Rock, C. O. (2012). Membrane disruption by antimicrobial fatty acids releases low-molecular-weight proteins from Staphylococcus aureus. *Journal of Bacteriology, 194*(19), 5294–5304. https://doi.org/10.1128/JB.00743-12

Pasqualone, A., Bianco, A. M., Paradiso, V. M., Summo, C., Gambacorta, G., & Caponio, F. (2014). Physico-chemical, sensory and volatile profiles of biscuits enriched with grape marc extract. *Food Research International, 65*, 385–393. https://doi.org/10.1016/j.foodres.2014.07.014

Passos, C. P., Yilmaz, S., Silva, C. M., & Coimbra, M. A. (2009). Enhancement of grape seed oil extraction using a cell wall degrading enzyme cocktail. *Food Chemistry, 115*(1), 48–53. https://doi.org/10.1016/j.foodchem.2008.11.064

Pérez, C., Ruiz Del Castillo, M. L., Gil, C., Blanch, G. P., & Flores, G. (2015). Supercritical fluid extraction of grape seeds: Extract chemical composition, antioxidant activity and inhibition of nitrite production in LPS-stimulated Raw 264.7 cells. *Food & Function, 6*(8), 2607–2613. https://doi.org/10.1039/C5FO00325C

Petrillo, A., Travaglioni, M., Di Fraia, S., Vanoli, L., Cirillo, D., & La Villetta, M. (2021). Experimental study and Life Cycle Assessment of biomass small-scale trigeneration plant. *Journal of Cleaner Production, 326*, Article 129234. https://doi.org/10.1016/j.jclepro.2021.129234

Polmann, G., Badia, V., Frena, M., Teixeira, G. L., Rigo, E., Block, J. M., & Camino Feltes, M. M. (2019). Enzyme-assisted aqueous extraction combined with experimental designs allow the obtaining of a high-quality and yield pecan nut oil. *Lebensmittel-Wissenschaft und -Technologie, 113*, Article 108283. https://doi.org/10.1016/j.lwt.2019.108283

Prezioso, I., Fioschi, G., Tufariello, M., Sanarica, L., Zara, I., Grieco, F., Di Fraia, A., Fiorentino, G., & Paradiso, V. M. (2026). Multienzyme engineering in the cellar: Versatile biotechnological potential of pectolytic-based clarification enzymes in rosé winemaking. *Food Bioscience, 76*, Article 108337. https://doi.org/10.1016/j.fbio.2026.108337

Rivero-Pino, F., León, M. J., Millán-Linares, M. C., & Montserrat-de la Paz, S. (2023). Antimicrobial plant-derived peptides obtained by enzymatic hydrolysis and fermentation as components to improve current food systems. *Trends in Food Science & Technology, 135*, 32–42. https://doi.org/10.1016/j.tifs.2023.03.005

Rosenthal, A., Pyle, D. L., & Niranjan, K. (1996). Aqueous and enzymatic processes for edible oil extraction. *Enzyme and Microbial Technology, 19*(6), 402–420. https://doi.org/10.1016/S0141-0229(96)80004-F

Salzano, F., Aulitto, M., Fiorentino, G., Cannella, D., Peeters, E., & Limauro, D. (2024). A novel endo-1,4-β-xylanase from Alicyclobacillus Mali FL18: Biochemical characterization and its synergistic action with β-xylosidase in hemicellulose deconstruction. *International Journal of Biological Macromolecules, 264*, Article 130550. https://doi.org/10.1016/j.ijbiomac.2024.130550

Samy, B. A., Raman, K., Velayutham, S., Senthilkumar, N., Thirumalaivasan, N., Kanagaraj, K., Pothu, R., Boddula, R., Radwan, A. B., & Al-Qahtani, N. (2025). Natural product extract fractions as potential arthritis treatments: A detailed analysis using in-silico, in-vivo, and in-vitro methods. *International Immunopharmacology, 144*, Article 113595. https://doi.org/10.1016/j.intimp.2024.113595

Santos-Silva, J., Bessa, R. J. B., & Santos-Silva, F. (2002). Effect of genotype, feeding system and slaughter weight on the quality of light lambs. *Livestock Production Science, 77*(2–3), 187–194. https://doi.org/10.1016/S0301-6226(02)00059-3

Sharma, D., Sharma, V., Tsai, M.-L., Nargotra, P., Yadav, A., Sun, P.-P., Chen, C.-W., & Dong, C.-D. (2025). Recent advances in ultrasound-assisted technologies for improved bioproduct recovery in lignocellulosic and microalgal biorefineries.

Journal of Industrial and Engineering Chemistry, 148, 38–51. https://doi.org/10.1016/j.jiec.2024.12.082

Spigno, G., Marinoni, L., & Garrido, G. D. (2017). State of the art in grape processing By-Products. In *Handbook of grape processing By-Products: Sustainable solutions* (pp. 1–27). https://doi.org/10.1016/B978-0-12-809870-7.00001-6

Sun, L., Wang, H., Wei, J., Xue, Y., Lan, S., Li, X., Yu, D., & Wang, J. (2022). Extracting oil from grape seed using a combined wet enzymatic process and pressing. *Innovative Food Science & Emerging Technologies, 77*, Article 102941. https://doi.org/10.1016/j.ifset.2022.102941

Thilakarathna, R. C. N., Siow, L. F., Tang, T.-K., & Lee, Y. Y. (2023). A review on application of ultrasound and ultrasound assisted technology for seed oil extraction. *Journal of Food Science and Technology, 60*(4), 1222–1236. https://doi.org/10.1007/s13197-022-05359-7

Thirumalaivasan, N., Kanagaraj, K., Nangan, S., Pothu, R., Rajendra, S. P., Karuppiah, P., & Boddula, R. (2025). Bioactive hydrogels (Bio- HyGs): Emerging trends in drug delivery and wound healing applications. *Polymers for Advanced Technologies, 36*(4), Article e70132. https://doi.org/10.1002/pat.70132

Thirumalaivasan, N., Nangan, S., Verma, D., Shellaiah, M., Ali, S., Rajendran, S., Kanagaraj, K., Pothu, R., Boddula, R., Radwan, A. B., & Al-Qahtani, N. (2025). Exploring the diverse nanomaterials employed in dental prosthesis and implant techniques: An overview. *Nanotechnology Reviews, 14*(1), Article 20250140. https://doi.org/10.1515/ntrev-2025-0140

Tociu, M., Hirtopeanu, A., & Stanescu, M. D. (2021). Enzymatic pre-treatment of grape seeds for an oil with higher antioxidant activity. *Grasas Y Aceites, 72*(4), Article e434. https://doi.org/10.3989/gya.1000202

Torabizadeh, H., & Khaki, L. (2025). Sesame oil and protein hydrolysates extraction by combined carbohydrases and proteases simultaneously in a single-unit aqueous-phase enzymatic bioreactor. *Food and Bioprocess Technology, 18*, 7330–7348. https://doi.org/10.1007/s11947-025-03872-z

Troilo, M., Difonzo, G., Paradiso, V. M., Pasqualone, A., & Caponio, F. (2022). Grape pomace as innovative flour for the formulation of functional muffins: How particle size affects the nutritional, textural and sensory properties. *Foods, 11*(12), 1799. https://doi.org/10.3390/foods11121799

Ulbricht, T. L. V., & Southgate, D. A. T. (1991). Coronary heart disease: Seven dietary factors. *The Lancet, 338*(8773), 985–992. https://doi.org/10.1016/0140-6736(91)91846-M

Verma, P., Kumar, A., Choudhary, R., Lai, C. W., Kaushik, R., & Wang, T. (2026). Recent progress in valorization of agro-food wastes in alignment with United Nations sustainable development goals. *International Journal of Environmental Science and Technology, 23*(2), 112. https://doi.org/10.1007/s13762-025-06856-w

Villacís-Chiriboga, J., Elíasdóttir, H. G., Badager, I., & Abdollahi, M. (2026). Impact of ultrasound–enzyme pretreatment sequence on recovery and functionality of proteins from an oat fiber-rich side stream. *Food Chemistry X, 33*, Article 103452. https://doi.org/10.1016/j.fochx.2025.103452

Voccia, D., Milvanni, G., Leni, G., & Lamastra, L. (2025). Life cycle assessment and circular economy evaluation of extraction techniques: Energy analysis of antioxidant recovery from wine residues. *Energies, 18*(18), 4851. https://doi.org/10.3390/en18184851

Vovk, H., Karnpakdee, K., Ludwig, R., & Nosenko, T. (2023). Enzymatic pretreatment of plant cells for oil extraction. *Food Technology and Biotechnology, 61*(2), 160–178. https://doi.org/10.17113/ftb.61.02.23.7896

Wang, D., Yuan, Y., Xie, T., Tang, G., Song, G., Li, L., Yuan, T., Zheng, F., & Gong, J. (2023). Ultrasound-assisted aqueous enzymatic extraction of gardenia fruits (Gardenia jasminoides Ellis) oil: Optimization and quality evaluation. *Industrial Crops and Products, 191*, Article 116021. https://doi.org/10.1016/j.indcrop.2022.116021

Wu, J., Johnson, L. A., & Jung, S. (2009). Demulsification of oil-rich emulsion from enzyme-assisted aqueous extraction of extruded soybean flakes. *Bioresource Technology, 100*(2), 527–533. https://doi.org/10.1016/j.biortech.2008.05.057

Yilmaz, E., Aydeniz Guneser, B., & Ok, S. (2019). Valorization of grapefruit seeds: Cold press oil production. *Waste and Biomass Valorization, 10*(9), 2713–2724. https://doi.org/10.1007/s12649-018-0286-x

Zhao, B., Gong, H., Li, H., Zhang, Y., Lan, T., & Chen, Z. (2019). Characterization of Chinese grape seed oil by physicochemical properties, fatty acid composition, triacylglycrol profiles, and sterols and squalene composition. *International Journal of Food Engineering, 15*(9), Article 20190031. https://doi.org/10.1515/ijfe-2019-0031

Zheng, C. J., Yoo, J.-S., Lee, T.-G., Cho, H.-Y., Kim, Y.-H., & Kim, W.-G. (2005). Fatty acid synthesis is a target for antibacterial activity of unsaturated fatty acids. *FEBS Letters, 579*(23), 5157–5162. https://doi.org/10.1016/j.febslet.2005.08.028

Zhu, M. J., Olsen, S. A., Sheng, L., Hu, J., Yue, W., & Means, W. J. (2015). Antimicrobial efficacy of grape seed extract against Escherichia coli O157:H7 growth, motility and Shiga toxin production. *Food Control, 51*, 177–182. https://doi.org/10.1016/j.foodcont.2014.11.024